Modeling of Reverse Curves on a Railway Line Using the Analytical Design Method

Wladyslaw Koc *

Posted Date: 4 December 2025

doi: 10.20944/preprints202512.0324.v1

Keywords: railway road; reverse curves; analytical design method; calculation algorithm; example geometric system

 doi:10.20944/preprints202512.0324.v1

Article

Modeling of Reverse Curves on a Railway Line Using the Analytical Design Method

Wladyslaw Koc

Faculty of Civil and Environmental Engineering, Gdansk University of Technology, 11/12 G. Narutowicza Str., 80-233 Gdansk, Poland; kocwl@pg.edu.pl

Abstract

The article deals with the issue of designing reverse curves in a railway track, i.e. a geometric system consisting of two circular arcs (usually with different radii), directed in opposite directions and directly connected to each other. It is also about being able to recreate (i.e. model) the existing geometric system with reverse arcs, so that it is then possible to correct the horizontal ordinates in the area where the circular arcs connect. An analytical method of designing track geometric systems was used, in which individual elements of these systems are described using mathematical equations. The design itself is carried out in the appropriate local Cartesian coordinate system, which is based on symmetrically arranged adjacent main directions of the route. The origin of this system is located at the point of intersection of adjacent main directions, whose coordinates in the global system are known. In the case of reverse curves, a third main direction appears, which significantly complicates the design procedure. The initial values of the radii of the reverse arcs must correspond to the existing system of main directions. The introduction of transition curves causes these radii to decrease; their values are determined iteratively. A set of formulas for creating a geometric system of reverse curves is presented. These formulas were used in the calculation example. A graph of the horizontal curvature of the track axis and a method for determining the possible train speed without the use of cant on an arc and with the use of cant are shown. The presented procedure is universal and can be applied to other geometric situations involving the design of reverse curves.

Keywords: railway road; reverse curves; analytical design method; calculation algorithm; example geometric system

1. Introduction

In the field of railways, the greatest interest is currently focused on high-speed railways (e.g., [1–5]). Numerous studies are also conducted on rolling stock and its maintenance (e.g., [6–8]. In the field of railway superstructure, the issue of interactions between the rail vehicle and the track system is being developed on a large scale (e.g., [9–13]).

When it comes to designing track layouts, there is a growing belief that conducting research on this topic is currently of lesser importance. This is undoubtedly due to the fact that for many years, design documentation for railways has been developed using commercial computer software [14,15]. While such work is certainly being conducted [16–19], its scope is often limited to specific issues such as transition curves [20–23] or railway turnouts [24–27].

Due to competitive conditions with other transportation systems, newly constructed railway lines are generally designed to accommodate increased train speeds; in fact, a significant portion of them are high-speed lines. However, the railway industry has a very long history. In terms of length, traditional lines, mostly built in the 19th century and still in operation today, still dominate. Undoubtedly, these lines would need to be adapted to modern requirements. This is particularly true for railway lines running through challenging terrain (e.g., mountainous terrain), which feature small horizontal arc radii and controversial geometric configurations, such as compound curves and reverse curves. Improving the quality of these lines, leading to increased travel speeds, requires

 doi:10.20944/preprints202512.0324.v1

appropriate modernization activities. Meanwhile, these lines seem to be disappearing from the research field.

This article addresses the design of reverse curves, a geometric arrangement consisting of two consecutive circular arcs (usually with different radii), oriented in opposite directions and directly connected. These curves have existed since the dawn of railway engineering, but they pose specific operational problems due to the rapid changes in curvature that occur. Subsequent advances in computational technology have also addressed them to a lesser extent. The design of reverse curves differs from other geometric arrangements in its level of complexity. From a scientific perspective, there is relatively little interest in this problem; rather, the practical aspects of the issue are exposed [28].

The goal was also to be able to recreate (i.e., model) the existing geometric system with reverse arcs, so that the horizontal ordinates in the area where the circular arcs connect could be corrected. An effective design method needed to be developed that could be used not only to determine the coordinates of the new reverse curve but also to model the existing system (with a view to its subsequent modification).

It should be noted here that an analytical method for designing reverse arcs had already been developed and presented in [29]. It involved a model solution, i.e., creating a geometric system from scratch in which reversely directed circular arcs of different radii are connected by an appropriate transition curve. The classic reverse arc, in which the transition curve does not occur, was a special case in this method. Modification of the existing geometric system was not considered. However, it seems that this is most often the real problem to be solved.

In this paper, the solution to the problem is achieved analytically. The standard procedure of the analytical design method requires operating in a local coordinate system. In its initial versions [30–32], it was characterized – in the initial phase – by a lack of knowledge of the origin of this system relative to the corresponding global coordinate system (in Poland – with respect to flat coordinates – this is the national spatial reference system PL-2000 [33]). Full integration of both systems requires the design procedure to be carried out in the local coordinate system until the very end. The location of the origin of this system relative to the corresponding main point of the route, and its resulting coordinates in the global coordinate system, were determined only in the final phase of the procedure. This could have been the fundamental methodological objection to the discussed design method. For this reason, certain interpretation problems could also arise.

As it turns out, these difficulties can be avoided by locating the origin of the local coordinate system at the intersection of two main directions of the route, whose Cartesian coordinates in the global system are known. This version of the analytical design method was presented in [34]; it is universal in nature and covers the areas where adjacent main directions of the railway route connect (both symmetrical and asymmetrical). In this paper, a similar approach was applied to the design of reverse curves.

However, reverse curves present a fundamental difference compared to most cases of analytical design method. In geometric systems, two adjacent main directions of the route are most often identified and further processed (including the creation of a local coordinate system). With reverse curves, a third main direction appears, significantly complicating matters by limiting the versatility of the developed method. However, when it comes to the local coordinate system, the adopted principle has been retained: it is determined using two adjacent principal directions.

To some extent, reference was made to the method of modeling compound curves on railway lines presented in [35]. However, the third main direction, which appears in the reverse arch, does not allow for a universal design method to be presented in symbolic notation, as is the case with compound curves. Therefore, in each stage of the entire procedure, appropriate theoretical formulas had to be directly applied to a specific calculation example. At the same time, the possibility of extending the scope of applications of the developed method through analogy was indicated.

 doi:10.20944/preprints202512.0324.v1

2. Layout of the Main Directions of the Route

When considering the horizontal plane of a railway line, the geometric arrangement of reverse curves includes three consecutive main directions (labeled *Line 1*, *Line 2*, and *Line 3*), with the last direction (*Line 3*) deviating from the preceding direction (*Line 2*) in the opposite direction. These directions intersect at points W_1 (*Line 1* with *Line 2*) and W_2 (*Line 2* with *Line 3*). Figure 1 shows an example of the geometric situation of these main directions in the PL-2000 system. This system has an easting coordinate axis *Y* and a northing coordinate axis *X*.

In the analytical method of designing track geometric systems [34], basic computational operations are performed in the local coordinate system *x*, *y*. This system is defined by two intersecting main directions, arranged symmetrically; their intersection point is the origin of the system in question. In the case of modeling reverse curves, it was decided to maintain this principle, determining the local coordinate system (*LCS*) based on the location of *Line 1* and *Line 2*. This is illustrated in Figure 1 by showing the position of the *LCS* axes in the PL-2000 system.

The equation of *Line 1* in the PL-2000 system is as follows:

$$X = X_{W1} + \tan\Phi_1 \left(Y - Y_{W1}\right), \tag{1}$$

and the equation of *Line 2* has the form:

$$X = X_{W1} + \tan\Phi_2 \left(Y - Y_{W1}\right), \tag{2}$$

where Y_{W1} and X_{W1} are the coordinates of point W_1, and Φ_1 and Φ_2 are the inclination angles of *Line 1* and *Line 2*, respectively.

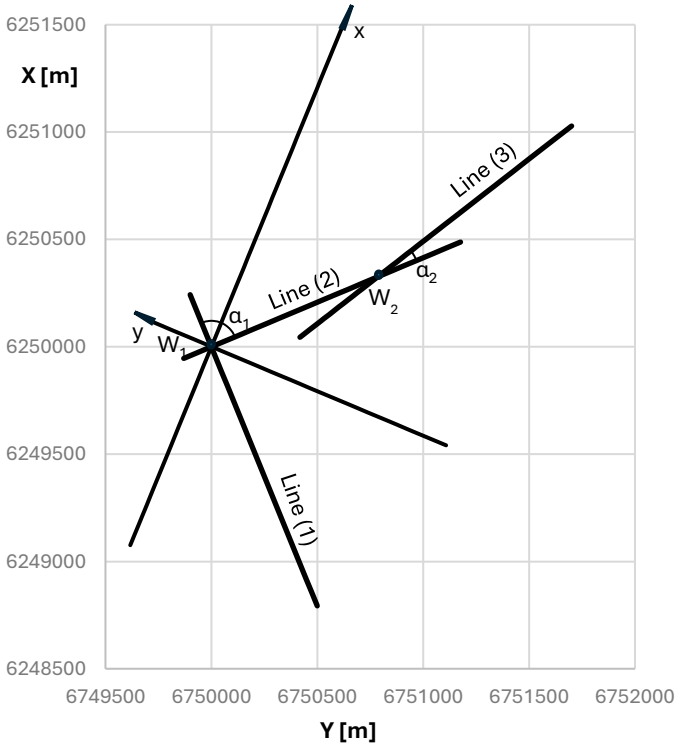

Figure 1. The layout of the main directions of the route in the PL-2000 system.

When adopting the appropriate numerical values in the calculation example, we were guided by the desire to obtain the greatest possible clarity of the geometric system in the *LCS*. Therefore, in this case, the coordinates of the main point Y_{W1} = 6,750,000 m, X_{W1} = 6,250,000 m and the slope of *Line 1* equal to $\Phi_1 = -3\pi/8$ rad were assumed. The assumed angle of return of the route $\alpha_1 = \pi/2$ rad results in the slope of *Line 2* equal to $\Phi_2 = \Phi_1 + \alpha_1 = \pi/8$ rad. The above data give the required values of the shifts Y_{W1} and X_{W1} and the rotation angle $\beta = \Phi_2 + \alpha_1/2 = 3\pi/8$ rad, leading to the transformation of

 doi:10.20944/preprints202512.0324.v1

coordinates from the PL-2000 system to the local coordinate system. This is performed using the following formulas [36]:

$$x = (Y - Y_{W1})\cos\beta - (X - X_{\partial W1})\sin\beta\,, \tag{3}$$

$$y = (Y - Y_{W1})\sin\beta + (X - X_{\partial W1})\cos\beta\,. \tag{4}$$

The angle of inclination of the x-axis in the PL-2000 system is $\Phi_x = \beta = 3\pi/8$ rad, so its equation is as follows:

$$X = X_{W1} + \tan\Phi_x\,(Y - Y_{W1})\,. \tag{5}$$

The angle of inclination of the y-axis in this system is equal to $\Phi_y = \beta - \pi/2 = -\pi/8$ rad; hence the equation of this axis

$$X = X_{W1} + \tan\Phi_y\,(Y - Y_{W1})\,. \tag{6}$$

Since the assumed angle of the route at point W_2 is equal to $\alpha_2 = \pi/12$ rad, the slope of *Line 3* is $\Phi_3 = \Phi_2 + \alpha_2 = \pi/6$ rad. From the point of view of operations carried out in the *LCS*, it turned out to be advantageous to adopt the coordinates of the next principal point Y_{W2} = 6,750,783.938 m and X_{W2} = 6,250,324.718 m. The given data result in the equation of *Line 3*:

$$X = X_{W2} + \tan\Phi_3\,(Y - Y_{W2})\,. \tag{7}$$

3. Local Coordinate System

It should be noted from the outset that the alignment of the main directions of the route in the PL-2000 coordinate system can vary greatly. However, after transformation to the local coordinate system, there are only two possible positions for the designed geometric system: under the x-axis, with negative ordinates and the convexity of the curvilinear elements directed upwards, and above the x-axis, with positive ordinates and the convexity of the curvilinear elements directed downwards [34]. Therefore, strictly speaking, both possible cases should be taken into account when determining the appropriate computational algorithms.

The main directions in Figure 1 indicate that in the *LCS* the geometric system under consideration lies below vertex W_1 and its ordinates are negative. This is the case that will be the subject of this article. The resulting formulas can also be applied to the system positioned above the x-axis, after making minor adjustments to the plus and minus signs.

The transfer of the route's main directions in Figure 1 to the local coordinate system is performed using formulas (3) and (4). This creates the situation shown in Figure 2.

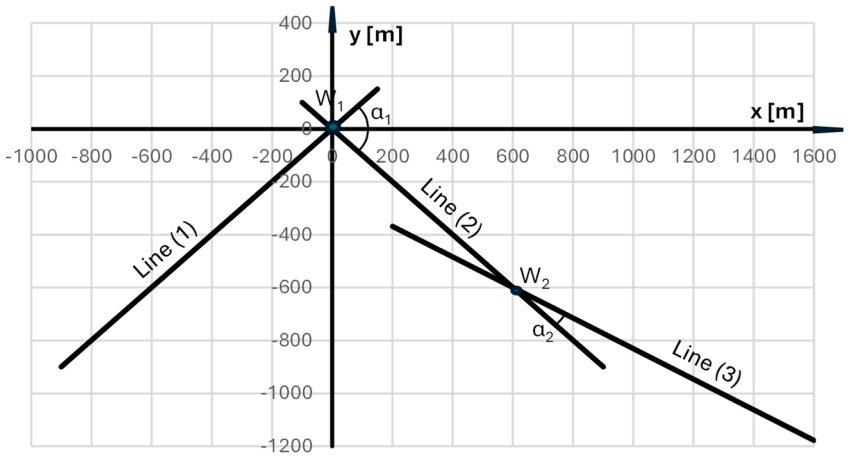

Figure 2. The system of main directions of the route in the local coordinate system.

 doi:10.20944/preprints202512.0324.v1

The origin of the local coordinate system, in which further detailed considerations will be conducted, is located at point $W_1(0,0)$, where *Line 1* and *Line 2* intersect. This is characteristic of the *LCS* used in the analytical method of designing geometric systems of the track [34].

The equations of the intersecting lines result from the angle of the route $\alpha 1$ for the first circular arc (marked as *Arc I*) and are as follows:

- for *Line 1*: $y = s_1 \cdot x$, $s_1 = \tan\varphi_1 = \tan\frac{\alpha_1}{2}$,
- for *Line 2*: $y = s_2 \cdot x$, $s_2 = \tan\varphi_2 = -\tan\frac{\alpha_1}{2}$,

where φ_1 and φ_2 are the inclination angles of *Line 1* and *Line 2* in the *LCS*. In the given case, the assumed turning angle is $\alpha_1 = \pi/2$ rad.

The second circular arc (marked as *Arc II*) is directed opposite to the preceding arc and connects *Line 2* with *Line 3*. Both lines intersect at point W_2, whose coordinates x_{W2} and y_{W2} result from the coordinates Y_{W2} and X_{W2}. The equation of *Line 3* results from the return angle α_2 for the second circular arc:

- $y = y_{W2} + s_3\left(x - x_{W2}\right)$, $s_3 = \tan\varphi_3 = \tan\left(-\frac{\alpha_1}{2} + \alpha_2\right)$.

where φ_3 is the angle of inclination of *Line 3* in the *LCS*. In the case under consideration, the coordinates of point W_2 are: $x_{W2} = 600$ m, $y_{W2} = -600$ m, and the angle of inclination of the line is equal to $\varphi_3 = -\pi/6$ rad.

As can be seen, the numerical parameters of the considered system of the main directions of the route in the *LCS* allow for convenient tracking of the design procedure, including, among others, defining individual geometric elements. After completing this procedure, the obtained solution is transferred to the PL-2000 system using transformation formulas [36]:

$$Y = Y_{W1} + x \cdot \cos\beta - y \cdot \sin\beta \,. \tag{8}$$

$$X = X_{W1} + x \cdot \sin\beta + y \cdot \cos\beta \,. \tag{9}$$

4. Reverse Arcs Radii

The values of the radii of the reverse arcs must correspond to the existing system of main directions. The key issue here is to choose the correct point of connection of both arcs. This point (marked *C* in Figure 2) is located on *Line 2*, and the condition $x_C \in \left(x_{W1}, x_{W2}\right)$ holds. For the assumed x_C, we determine y_C using the formula

$$y_C = -\left(\tan\frac{\alpha_1}{2}\right)x_C \,. \tag{10}$$

Then we calculate the distances $\overline{W_1C}$ and $\overline{CW_2}$.

$$\overline{W_1C} = \sqrt{\left(x_C - x_{W1}\right)^2 + \left(y_C - y_{W1}\right)^2} \,, \tag{11}$$

$$\overline{CW_2} = \sqrt{\left(x_{W2} - x_C\right)^2 + \left(y_{W2} - y_C\right)^2} \,. \tag{12}$$

Of course, the condition must be met

$$\overline{W_1C} + \overline{CW_2} = \overline{W_1W_2} = \sqrt{\left(x_{W2} - x_{W1}\right)^2 + \left(y_{W2} - y_{W1}\right)^2} \,.$$

We treat $\overline{W_1C}$ and $\overline{CW_2}$ as tangents of the corresponding reverse circular arcs. First, we determine the radius $R_{(I)}$ of *Arc I*. Since its angle of return is $\alpha_1 = \left|\varphi_2 - \varphi_1\right|$, for $\varphi_1 = \pi/4$ rad, $\varphi_2 = -\pi/4$ rad, we obtain $\alpha_1 = \pi/2$ rad. From the formula for the value of the tangent

 doi:10.20944/preprints202512.0324.v1

$$t_1 = \overline{W_1 C} = \left(\tan \frac{|\varphi_2 - \varphi_1|}{2} \right) R_{(I)} \tag{13}$$

it follows that

$$R_{(I)} = \frac{t_1}{\tan \frac{|\varphi_2 - \varphi_1|}{2}} \quad . \tag{14}$$

The return angle of *Arc II*, with radius $R_{(II)}$, is $\alpha_2 = |\varphi_3 - \varphi_2|$. Since in the case under consideration $\varphi_2 = -\pi/4$ rad, $\varphi_3 = -\pi/6$ rad, we obtain $\alpha_2 = \pi/12$ rad. The formula for the value of the tangent is

$$t_2 = \overline{C W_2} = \left(\tan \frac{|\varphi_3 - \varphi_2|}{2} \right) R_{(II)} \quad , \tag{15}$$

hence

$$R_{(II)} = \frac{t_2}{\tan \frac{|\varphi_3 - \varphi_2|}{2}} \quad . \tag{16}$$

Table 1 presents the values of the radii of the reverse arcs determined for different coordinates of point *C* in the considered calculation example.

Table 1. Example values of radii $R_{(I)}$ and $R_{(II)}$ for different coordinates of point *C*.

Abscissa x_C **[m]**	**Ordinate** y_C **[m]**	**Tangent** t_1 **[m]**	**Radius** $R_{(I)}$ **[m]**	**Tangent** t_2 **[m]**	**Radius** $R_{(II)}$ **[m]**
350	– 350	494.075	494.975	353.553	2685.505
375	– 375	530.330	530.330	318.198	2416.954
400	– 400	565.685	565.685	282.843	2348.404
425	– 425	601.041	601.041	247.487	1879.853
450	**– 450**	**636.396**	**636.396**	**212.132**	**1611.303**
475	– 475	671.751	671.751	176.777	1342.752
500	– 500	707.107	707.107	141.421	1074.202

As can be seen, for a given arrangement of the main directions of the route and the assumed location of the circular arc connection, there is a specific relationship between the values of these arc radii. Therefore, reverse arcs cannot be shaped arbitrarily; various conditions must be taken into account. Based on the data from Table 1, the case x_C = 450 m, y_C = –450 m (bold) was qualified for further analysis. This meant that considerations had to be conducted for the initial values of the circular arc radii $R_{(I)}$ = 636.396 m and $R_{(II)}$ = 1611.303 m.

 doi:10.20944/preprints202512.0324.v1

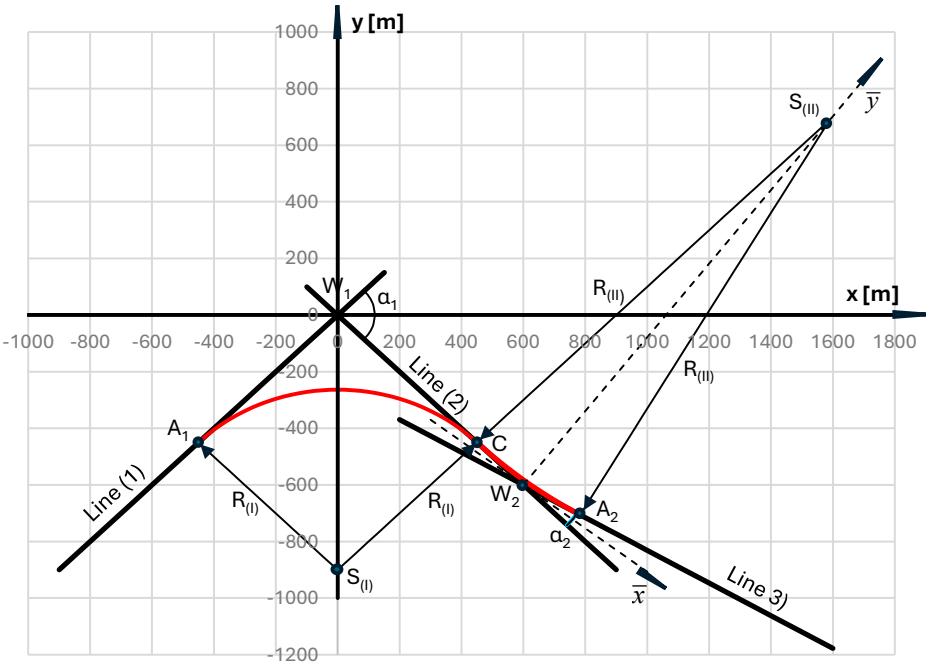

Figure 3. The primary geometric arrangement of reverse arcs in the local coordinate system.

Entering the designated arcs into the system of main directions allows us to create the original geometric system of reverse arcs. This requires first determining the coordinates of the starting point A_1 for the arc with radius $R_{(I)}$ and the ending point A_2 for the arc with radius $R_{(II)}$ (Figure 3). The coordinates of the point where both arcs join (i.e., point C) are already known.

The following formulas apply:

$$x_{A1} = x_{W1} - \frac{1}{\sqrt{1+s_1^2}} t_1 \quad , \tag{17}$$

$$y_{A1} = y_{W1} - \frac{s_1}{\sqrt{1+s_1^2}} t_1 \quad , \tag{18}$$

$$x_{A2} = x_{W2} + \frac{1}{\sqrt{1+s_3^2}} t_2 \quad , \tag{19}$$

$$y_{A2} = y_{W2} - \frac{s_3}{\sqrt{1+s_3^2}} t_2 \quad . \tag{20}$$

In the case shown in Figure 3, the determined coordinates are as follows: $x_{A1} = -450$ m, $y_{A1} = -450$ m, $x_{A2} = 783.712$ m and $y_{A2} = -706.066$ m.

In the next step, the coordinates of the centers of both circular arcs are determined. For *Arc I*, lines perpendicular to the corresponding main directions are drawn from points A_1 and C. The center of the arc $S_{(I)}$ lies at the intersection of these lines. After solving the appropriate system of equations, the formulas for its coordinates are obtained:

$$x_{S(I)} = \frac{s_1 s_2}{s_2 - s_1} \left(\frac{1}{s_1} x_{A1} - \frac{1}{s_2} x_C + y_{A1} - y_C \right) \quad , \tag{21}$$

$$y_{S(I)} = y_{A1} - \frac{1}{s_1} \left(x_{S(I)} - x_{A1} \right) \quad , \tag{22a}$$

 doi:10.20944/preprints202512.0324.v1

$$y_{S(I)} = y_C - \frac{1}{s_2}\left(x_{S(I)} - x_C\right) \quad . \tag{22b}$$

The equation of *Arc I* is as follows:

$$y = y_{S(I)} \pm \sqrt{R_{(I)}^2 - \left(x - x_{S(I)}\right)^2} \quad . \tag{23}$$

In the case under consideration $x_{S(I)} = 0$, $y_{S(I)} = -900$ m, and the arc equation has the form

$$y = -900 + \sqrt{(636.396)^2 - x^2} \quad , \qquad x \in \langle -450; 450 \rangle \text{ m}.$$

The procedure for *Arc II* is analogous. Lines perpendicular to the corresponding main directions are drawn from points *C* and A_2. After solving the appropriate system of equations, the formulas for the coordinates of the center of the arc $S_{(II)}$ are obtained:

$$x_{S(II)} = \frac{s_2 s_3}{s_3 - s_2}\left(\frac{1}{s_2}x_C - \frac{1}{s_3}x_{A2} + y_C - y_{A2}\right) \quad , \tag{24}$$

$$y_{S(II)} = y_C - \frac{1}{s_2}\left(x_{S(II)} - x_C\right) \quad , \tag{25a}$$

$$y_{S(II)} = y_{A2} - \frac{1}{s_3}\left(x_{S(II)} - x_{A2}\right) \quad , \tag{25b}$$

The equation of *Arc II* has the following form:

$$y = y_{S(II)} \pm \sqrt{R_{(II)}^2 - \left(x - x_{S(II)}\right)^2} \quad . \tag{26}$$

In the case under consideration $x_{S(II)} = 1589.363$ m, $y_{S(II)} = 689.363$ m, and the arc equation is as follows:

$$y = 689.363 - \sqrt{(1611.303)^2 - (x - 1589.363)^2} \quad , \qquad x \in \langle 450; 783.712 \rangle \text{ m}.$$

The inserted reverse arcs are marked in red in Figure 3. The $\bar{x}, \bar{y}$ auxiliary coordinate system is also shown there, which will be used to analyze the application of transition curves for *Arc II* (in Chapter 7).

5. Curvature of the Primary Reverse Arc System

The arrangement of primary reverse curves shown in Figure 3 raises serious concerns. These arise from the occurrence of very unfavorable lateral accelerations when the rail vehicle is traveling at a given speed *V*. This is best seen in the curvature diagram of the geometric system, from which these accelerations directly result.

To determine the curvature graph along the length of the geometric system, a rail vehicle model was used in the form of its rigid base with a length of l_b = 20 m. The curvature value is obtained by tracking the position of the moving center of the rigid base. Figure 4 shows the curvature graph obtained for the system of reverse arcs from Figure 3.

 doi:10.20944/preprints202512.0324.v1

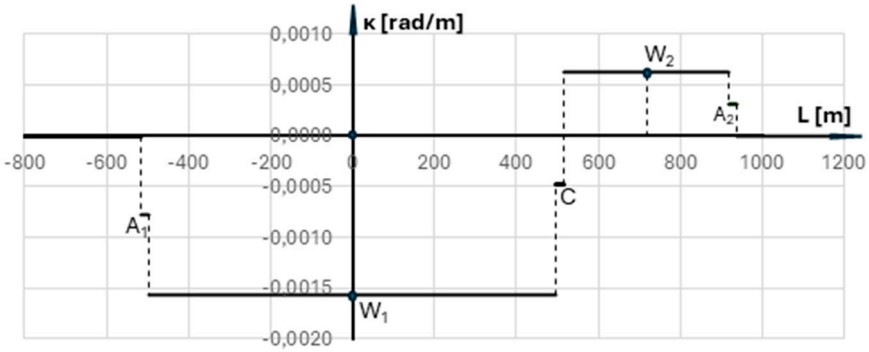

Figure 4. Curvature diagram over the length of the primary reverse arc system.

As can be seen in the graph, there are sudden, abrupt changes in curvature around points A_1, C, and A_2. This causes two impacts at each point, transverse to the track, which can be easily observed, for example, on tram lines. However, travel on these lines in the areas of abrupt changes in curvature is usually very slow. On railway lines, much higher speeds apply, meaning travel times are shorter, and therefore the impact-mitigating effect of the rigid base is limited. Therefore, from a theoretical perspective, travel on the discussed geometric configuration could be achieved at low speeds.

Because in real track, due to its stiffness, the curvature at the joints of individual geometric elements is smoothed out, certain simplifying assumptions can be made to estimate the possible train speed. This involves the assumption (which is highly debatable, by the way) that the change in curvature at critical points occurs not abruptly, but linearly along the length of the rigid base.

The velocity on the geometric system of reverse curves results from the situation occurring at point C, i.e., at the point of contact of *Arc I* and *Arc II*. These are curves without cant (i.e., $h_1 = 0$ and $h_2 = 0$). The values of unbalanced acceleration, directed in opposite directions, are as follows:

$$a_{m1} = \frac{V^2}{(3.6)^2 R_{(I)}} \quad , \qquad a_{m2} = \frac{V^2}{(3.6)^2 R_{(II)}} \quad ,$$

where the velocity V is expressed in km/h, the radii $R_{(I)}$ and $R_{(II)}$ R(I) in meters, and the accelerations a_{m1} and a_{m2} in m/s².

According to Polish regulations [37], acceleration values should be less than $a_{per} = 0.85$ m/s², but this condition is insufficient. The acceleration increase condition should also be checked:

$$\psi = \frac{(a_{m1} + a_{m2}) \cdot V}{3.6 \cdot l_b} \le \psi_{per}$$

for the assumed length of the rigid wagon base, where ψ is expressed in m/s³. The acceleration increase should be smaller than $\psi_{per} = 0.5$ m/s³ [38]. The relevant analysis is presented in Table 2.

Table 2. Determining the approximate train speed for the original reverse curves system..

Train speed V [km/h]	Radius $R_{(I)}$ [m]	Acceleration a_{m1} [m/s²]	Radius $R_{(II)}$ [m]	Acceleration a_{m2} [m/s²]	Sum of accelerations $a_{m1} + a_{m2}$ [m/s²]	Acceleration increase ψ [m/s³]
50	636.396	0.303115	1611.303	0.119718	0.422833	0.293634
55	636.396	0.366769	1611.303	0.144858	0.511627	0.390827
60	636.396	0.436486	1611.303	0.172393	0.608879	**0.507399**
65	636.396	0.512264	1611.303	0.202323	0.714587	0.645113
70	636.396	0.594105	1611.303	0.234646	0.828752	0.805731

In the case under consideration, this gives a speed of $V_{max} = 60$ km/h (shown in bold in Table 2). This speed is relatively low and, moreover, not entirely reliable. Therefore, modeling of reverse

 doi:10.20944/preprints202512.0324.v1

curves should be continued by introducing transition curves for both existing circular arcs. This is possible if there is an appropriate distance between vertices W_1 and W_2 (it cannot be too small).

The transition curves are entered separately for *Arc I* and *Arc II*. As a result of this operation the radii of these arcs are reduced. The corresponding calculation procedure for *Arc I* is performed in the local coordinate system, while for *Arc II* in the $\bar{x}, \bar{y}$ auxiliary coordinate system, with subsequent transfer of the obtained solution to the *LCS*.

6. Applying Transition Curves for the First Circular Arc

For *Arc I*, with the primary (initial) radius $R_{(I)}$, transition curves of different lengths $L_{(I)i}$, $i = 1, 2, \ldots$ can be used. Figure 5 shows a fragment of the local coordinate system containing the effects of using symmetric transition curves of length 50 m and 100 m. The initial geometric system is marked in red, the system with curves of length $L_{(I)1} = 50$ m is marked in green, and the system with curves of length $L_{(I)2} = 100$ m is marked in purple.

The given task is to introduce transition curves p and q in the form of a clothoid with an assumed, differentiated length $L_{(I)i}$ at both ends of *Arc I* (i.e. originating from points A_1 and C). Since the designed geometric system is symmetrical, it is sufficient to consider in detail one (in this case the left) half of it (i.e. with transition curve p). The straight segment on the left side of the system (i.e., *Line 1*) is the abscissa axis of the Cartesian coordinate system x_k, y_k, associated with the given transition curve. The origin of this system is at point A_1. We are interested in the coordinates of the curve's endpoint (i.e., point $K_{p(I)i}$) in this system; they result from the corresponding parametric equations $x_k(l)$ and $y_k(l)$ for $l = L_{(I)i}$. Since – as it turns out – we must take into account the need to correct the radius of the circular arc, the transition curve equations must use different values of the arc radius $R_{(I)i}$. When using a transition curve in the form of a clothoid, the following parametric equations apply in the x_k, y_k system:

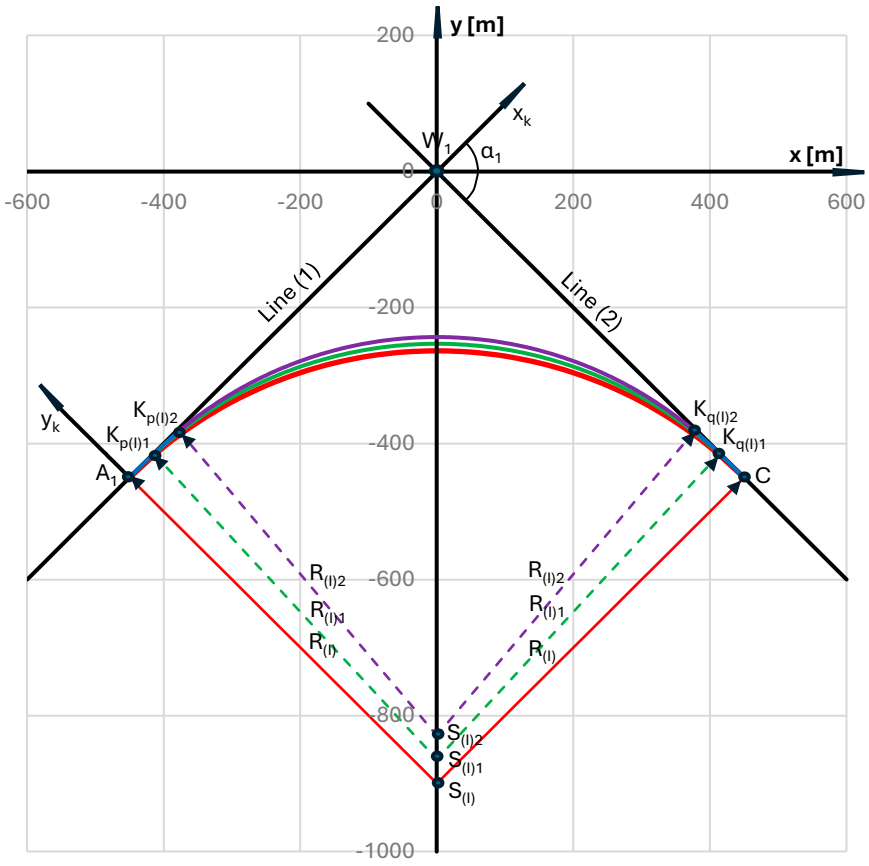

Figure 5. Effects of using symmetrical transition curves of 50 m and 100 m length for *Arc I* (in the local coordinate system).

 doi:10.20944/preprints202512.0324.v1

$$x_k(L_{(I)i}) = L_{(I)i} - \frac{L_{(I)i}^3}{40 \cdot R_{(I)i}^2} + \frac{L_{(I)i}^5}{3,456 \cdot R_{(I)i}^4} \quad , \tag{27}$$

$$y_k(L_{(I)i}) = -\frac{L_{(I)i}^2}{6 \cdot R_{(I)i}} + \frac{L_{(I)i}^4}{336 \cdot R_{(I)i}^3} - \frac{L_{(I)i}^6}{42,240 \cdot R_{(I)i}^5} \quad , \tag{28}$$

while the angle of inclination $\Theta_k(L_{(I)i})$ at the end of the curve is determined from the relationship

$$\Theta_k(L_{(I)i}) = -\frac{L_{(I)i}}{2 \cdot R_{(I)i}} \quad . \tag{29}$$

The transformation of the transition curve to the x, y coordinate system is performed by rotating the reference system by an angle of $\alpha_1/2$ and shifting the curve origin to point A_1. The corresponding formulas depend on the direction of rotation. This operation yields the desired values of the transition curve projections onto the horizontal and vertical axes, which are the coordinates of the curve's endpoint. If the x_k, y_k system is rotated clockwise (as in Figure 5), the following relations are obtained:

$$x_{Kp(I)i} = x(L_{(I)i}) = x_{A1} + x_k(L_{(I)i}) \cdot \cos\frac{\alpha_1}{2} - y_k(L_{(I)i}) \cdot \sin\frac{\alpha_1}{2} \quad , \tag{30}$$

$$y_{Kp(I)i} = y(L_{(I)i}) = y_{A1} + x_k(L_{(I)i}) \cdot \sin\frac{\alpha_1}{2} + y_k(L_{(I)i}) \cdot \cos\frac{\alpha_1}{2} \quad . \tag{31}$$

The angle of inclination $\Theta(L_{(I)i})$ at the end of the curve is determined from the formula

$$\Theta_{Kp(I)i} = \Theta(L_{(I)i}) = -\frac{L_{(I)i}}{2 \cdot R_{(I)i}} + \frac{\alpha_1}{2} \quad . \tag{32}$$

Since the introduction of this transition curve is performed while maintaining the position of its starting point (i.e. point A_1), it is necessary to correct the position of the circular arc so that it starts at the point with coordinates $x_{Kp(I)i}$ and $y_{Kp(I)i}$, the angle of inclination of the tangent is $\Theta_{Kp(I)i}$ and the condition of symmetry of the entire system is met (i.e. $\Theta(0) = 0$). This is illustrated in the situation shown in Figure 5.

In this situation, the condition $\Theta(0) = 0$ requires a correction of the arc radius value. This is directly related to the assumed transition curve length. The final solution to the problem is achieved for a specific value of $L_{(I)i}$, which is considered the most favorable.

Determining the corrected radius $R_{(I)i}$ requires determining the coordinates of the center $S_{(I)i}$ of the corresponding circular arc. It lies on the line perpendicular to the tangent at the end of the transition curve, with the equation

$$y(x) = y_{Kp(I)i} - \frac{1}{\tan\Theta_{Kp(I)i}}\left(x - x_{Kp(I)i}\right) \quad ,$$

at a distance $R_{(I)i}$ from the point $K_{p(I)i}$; it follows from this

$$\sqrt{\left(x_{S(I)i} - x_{Kp(I)i}\right)^2 + \left(y_{S(I)i} - y_{Kp(I)i}\right)^2} = R_{(I)i} \, .$$

By solving the appropriate system of equations, we obtain the desired coordinates

$$x_{S(I)i} = x_{Kp(I)i} + \frac{\tan\Theta_{Kp(I)i}}{\sqrt{1 + \left(\tan\Theta_{Kp(I)i}\right)^2}} R_{(I)i} \quad , \tag{33}$$

$$y_{S(I)i} = y_{Kp(I)i} - \frac{1}{\sqrt{1 + \left(\tan\Theta_{Kp(I)i}\right)^2}} R_{(I)i} \quad . \tag{34}$$

 doi:10.20944/preprints202512.0324.v1

The necessity of fulfilling the condition $x_{S(I)i} = 0$ means that

$$R_{(I)i} = -\frac{\sqrt{1+\left(\tan\Theta_{Kp(I)i}\right)^2}}{\tan\Theta_{Kp(I)i}} x_{Kp(I)i} \quad , \tag{35}$$

determining the coordinates of point $S_{(I)i}$ with a changing value of this radius.

The basic criterion for solving the problem is to meet the key condition $x_{S(I)i} = 0$. The final part of the calculations for the selected case (with $\alpha_1 = \pi/2$ rad, $x_{A1} = -450$ m, $y_{A1} = -450$ m and $L_{(I)1} = 50$ m) is shown in Table 3.

Taking into account the appropriate number of decimal places for the determined abscissa $x_{S(I)1}$ indicated the corrected circular arc radius $R_{(I)1} = 611.227$ m (marked in bold in Table 3). Thus, the circular arc of radius $R_{(I)}$, which is part of the reverse arc, is replaced by a circular arc of radius $R_{(I)1}$ and two transition curves of length $L_{(I)1} = 50$ m (Figure 5).

Table 3. Determining the corrected radius of the first arc for $L_{(I)1} = 50$ m.

Radius $R_{(I)1}$ [m]	Abscissa $x_k(L_{(I)1})$ [m]	Ordinate $y_k(L_{(I)1})$ [m]	Angle $\Theta_k(L_{(I)1})$ [rad]	Abscissa $x_{Kp(I)1}$ [m]	Ordinate $y_{Kp(I)1}$ [m]	Angle $\Theta_{Kp(I)1}$ [rad]	Abscissa $x_{S(I)1}$ [m]	Ordinate $y_{S(I)1}$ [m]
611.230	49.99164	-0.68160	0.0409	-414.169	-415.133	0.744497	0.002060594	-864.649
611.229	49.99164	-0.68161	0.0409	-414.169	-415.133	0.744497	0.001353681	-864.648
611.228	49.99164	-0.68161	0.0409	-414.169	-415.133	0.744497	0.000646768	-864.647
611.227	49.99164	-0.68161	0.0409	-414.169	-415.133	0.744497	**-0.00006014**	**-864.647**
611.226	49.99164	-0.68161	0.0409	-414.169	-415.133	0.744497	-0.00076706	-864.646
611.225	49.99164	-0.68161	0.0409	-414.169	-415.133	0.744497	-0.00147397	-864.645
611.224	49.99164	-0.68161	0.0409	-414.169	-415.133	0.744497	-0.00218088	-864.644
611.223	49.99164	-0.68161	0.0409	-414.169	-415.133	0.744497	-0.00288780	-864.644
611.222	49.99164	-0.68161	0.0409	-414.169	-415.133	0.744496	-0.00359471	-864.643

The general equation of a circular arc with radius $R_{(I)i}$ has the form

$$y = y_{S(I)i} + \sqrt{R_{(i)i}^2 - x^2} \quad , \qquad x \in \left\langle x_{Kp(I)i}, x_{Kq(I)i} \right\rangle \quad . \tag{36}$$

Taking into account the existing symmetry, the entire arrangement of the first arc is described as follows:

- for $x \in \left\langle x_{A1}, x_{Kp(I)i} \right\rangle$, that is $l \in \left\langle 0, L_{(I)i} \right\rangle$

$$x(l) = x_{A1} + x_k(l) \cdot \cos\frac{\alpha_1}{2} - y_k(l) \cdot \sin\frac{\alpha_1}{2} \quad ,$$

$$y(l) = y_{A1} + x_k(l) \cdot \sin\frac{\alpha_1}{2} + y_k(l) \cdot \cos\frac{\alpha_1}{2} \quad ,$$

where

$$x_k(l) = l - \frac{l^5}{40 \cdot R_{(I)i}^2 \cdot L_{(I)i}^2} + \frac{l^9}{3{,}456 \cdot R_{(I)i}^4 \cdot L_{(I)i}^4} \quad ,$$

$$y_k(l) = -\frac{l^3}{6 \cdot R_{(I)i} \cdot l_{(I)i}} + \frac{l^7}{336 \cdot R_{(I)i}^3 \cdot L_{(I)i}^3} - \frac{l^{11}}{42{,}240 \cdot R_{(I)i}^5 \cdot L_{(I)i}^5} \quad .$$

- for $x \in \left\langle x_{Kp(I)i}, x_{Kq(I)i} \right\rangle$, where $x_{Kq(I)i} = -x_{Kp(I)i}$

$$y = y_{S(I)i} + \sqrt{R_{(I)i}^2 - x^2} \quad .$$

- for $x \in \left\langle x_{Kq(I)i}, x_C \right\rangle$, that is $l \in \left\langle -L_{(I)i}, 0 \right\rangle$

 doi:10.20944/preprints202512.0324.v1

$$x(l) = x_C + x_k(l) \cdot \cos\frac{\alpha_1}{2} + y_k(l) \cdot \sin\frac{\alpha_1}{2} \quad ,$$

$$y(l) = y_C - x_k(l) \cdot \sin\frac{\alpha_1}{2} + y_k(l) \cdot \cos\frac{\alpha_1}{2} \quad .$$

where

$$x_k(l) = l - \frac{l^5}{40 \cdot R_{(I)i}^2 \cdot L_{(I)i}^2} + \frac{l^9}{3,456 \cdot R_{(I)i}^4 \cdot L_{(I)i}^4} \quad ,$$

$$y_k(l) = \frac{l^3}{6 \cdot R_{(I)i} \cdot L_{(I)i}} - \frac{l^7}{336 \cdot R_{(I)i}^3 \cdot L_{(I)i}^3} + \frac{l^{11}}{42,240 \cdot R_{(I)i}^5 \cdot L_{(I)i}^5} \quad .$$

In the situation shown in Figure 5, $L_{(I)1}$ = 50 m was first assumed. Since $\alpha_1 = \pi/2$ rad, x_{A1} = –450 m and y_{A1} = –450 m, the coordinates of the end of the first transition curve in the x_k, y_k system are as follows: $x_k(L_{(I)1})$ = 49.992 m, $y_k(L_{(I)1})$ = –0.665 m. The angle of inclination of the tangent is $\Theta(L_{(I)1})$ = –0.03928 rad. The coordinates of the center of the corrected arc are: $x_{S(I)1}$ = 0, $y_{S(I)1}$ = –864.647 m. This corresponds to the following values in the local coordinate system: $x_{Kp(I)1}$ = –414.187 m, $y_{Kp(I)1}$ = –415.113 m, $\Theta_{Kp(I)1}$ = 0.746114 rad, $x(0)$ = 0, $y(0)$ = –253.420 m, $x_{Kq(I)1}$ = 414.187 m, $y_{Kq(I)1}$ = –415.113 m, $\Theta_{Kq(I)1}$ = –0.746114 rad, x_C = 450 m and y_C = –450 m. The entire geometric system is shown in Figure 5 (the circular arc is marked in green).

The next step was to assume the length $L_{(I)2}$ = 100 m (while maintaining $\alpha_1 = \pi/2$ rad, x_{A1} = –450 m, and y_{A1} = –450 m). As before, the radius $R_{(I)2}$ should be determined numerically by specifying the coordinates of point $S_{(I)2}$ with varying values of this radius. The basic criterion for solving the problem is to meet the key condition $x_{S(I)2}$ = 0. The final part of the calculations for the discussed case is shown in Table 4.

Table 4. Determining the corrected radius of the first curve for $L_{(I)2}$ = 100 m.

Radius $R_{(I)2}$ [m]	Abscissa $x_k(L_{(I)2})$ [m]	Ordinate $y_k(L_{(I)2})$ [m]	Angle $\Theta_k(L_{(I)2})$ [rad]	Abscissa $x_{Kp(I)2}$ [m]	Ordinate $y_{Kp(I)2}$ [m]	Angle $\Theta_{Kp(I)2}$ [rad]	Abscissa $x_{S(I)2}$ [m]	Ordinate $y_{S(I)2}$ [m]
585.694	99.92715	-2.84415	-0.08537	-377.330	-381.352	0.700029	-0.00213926	-829.304
585.695	99.92715	-2.84414	-0.08537	-377.330	-381.352	0.700029	-0.00143299	-829.305
585.696	99.92715	-2.84414	-0.08537	-377.330	-381.352	0.700030	-0.00072671	-829.306
585.697	99.92715	-2.84413	-0.08537	-377.330	-381.352	0.700030	**-0.00002043**	**-829.306**
585.698	99.92715	-2.84413	-0.08537	-377.330	-381.352	0.700030	0.00068585	-829.307
585.699	99.92715	-2.84412	-0.08537	-377.330	-381.352	0.700030	0.00139212	-829.308
585.700	99.92715	-2.84412	-0.08537	-377.330	-381.352	0.700030	0.00209840	-829.309

Taking into account the appropriate number of decimal places for the determined abscissa $x_{S(I)2}$ indicates a corrected circular arc radius $R_{(I)2}$ = 585.697 m (marked in bold in Table 4). Thus, the circular arc of radius $R_{(I)}$, which is part of the reverse arc, is replaced by a circular arc of the given radius and two transition curves of 100 m length. This is shown in Figure 5, where the circular arc is marked in purple.

The coordinates of the end of the first transition curve in the x_k, y_k system are as follows: $x_k(L_{(I)2})$ = 99.927 m, $y_k(L_{(I)2})$ = –2.844 m. The angle of inclination of the tangent is $\Theta(L_{(I)2})$ = –0.085368 rad. The coordinates of the center of the corrected arc are: $x_{S(I)2}$ = 0, $y_{S(I)2}$ = –829.306 m. This corresponds to the following values in the local coordinate system: $x_{Kp(I)2}$ = –377.330 m, $y_{Kp(I)2}$ = –381.352 m, $\Theta_{Kp(I)2}$ = 0.70003 rad, $x(0)$ = 0, $y(0)$ = –243.609 m, $x_{Kq(I)2}$ = 377.330 m, $y_{Kq(I)2}$ = –381.352 m, $\Theta_{Kq(I)2}$ = –0.70003 rad, x_C = 450 m and y_C = –450 m.

 doi:10.20944/preprints202512.0324.v1

7. Applying Transition Curves for the Second Circular Arc

The transition curves at *Arc II* (with radius $R_{(II)}$) are inserted in the $\bar{x},\bar{y}$ auxiliary coordinate system (Figure 3). This system has its origin at point W_2, and the ordinate axis on the line passing through points W_2 and $S_{(II)}$. The equation of the axes in the *LCS* is as follows:

$$y = y_{W2} + \frac{y_{S(II)} - y_{W2}}{x_{S(II)} - x_{W2}}\left(x - x_{W2}\right) \quad . \tag{37}$$

The $\bar{x}$ axis passes through point W_2 perpendicularly to the $\bar{y}$ axis; therefore, it is described by the equation

$$y = y_{W2} - \frac{x_{S(II)} - x_{W2}}{y_{S(II)} - y_{W2}}\left(x - x_{W2}\right) \quad . \tag{38}$$

The separated auxiliary coordinate system is shown in Figure 6. It contains the effects of applying symmetrical transition curves in the form of a clothoid for an arc with an initial radius $R_{(II)}$. The primary geometric system (without transition curves) is marked in red, which, however – in the adopted drawing scale – has been obscured by the system with curves of length $L_{(II)1}$ = 50 m, marked in purple.

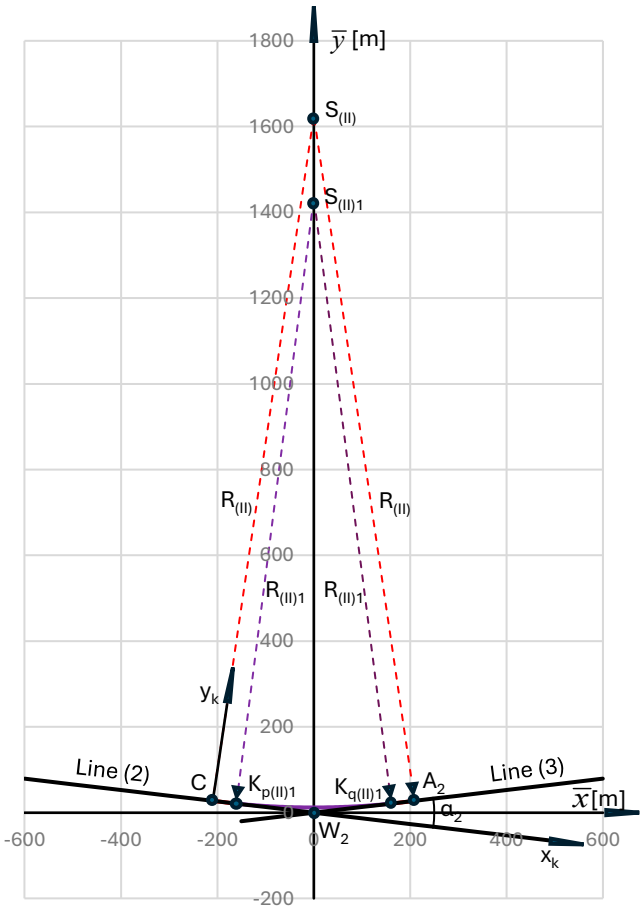

Figure 6. A circular arc with a larger radius (located between points *C* and A_2), corrected by introducing transition curves (marked in purple).

In the $\bar{x},\bar{y}$ system, the inclinations of the main directions intersecting at point $W_2(0,0)$ result from the angle of inclination α_2. The angle of inclination of *Line 2* is $-\alpha_2/2$, and of *Line 3*: $\alpha_2/2$. The abscissa of point $S_{(II)}$ is equal to zero, and the ordinate results from the relationship:

 doi:10.20944/preprints202512.0324.v1

$$\bar{y}_{S(II)} = \sqrt{\left(x_{S(II)} - x_{W2}\right)^2 + \left(y_{S(II)} - y_{W2}\right)^2} \quad . \tag{39}$$

Point *C* has coordinates:

$$\bar{x}_C = -R_{(II)} \cos\frac{\alpha_2}{2} \tan\frac{\alpha_2}{2} \quad , \tag{40}$$

$$\bar{y}_C = R_{(II)} \sin\frac{\alpha_2}{2} \tan\frac{\alpha_2}{2} \quad , \tag{41}$$

and point A_2:

$$\bar{x}_{A2} = R_{(II)} \cos\frac{\alpha_2}{2} \tan\frac{\alpha_2}{2} \quad , \tag{42}$$

$$\bar{y}_{A2} = R_{(II)} \sin\frac{\alpha_2}{2} \tan\frac{\alpha_2}{2} \quad . \tag{43}$$

The equation of *Line 2* has the form

$$\bar{y} = -\left(\tan\frac{\alpha_2}{2}\right) \cdot \bar{x} \quad , \tag{44}$$

and the equation of *Line 3*

$$\bar{y} = \left(\tan\frac{\alpha_2}{2}\right) \cdot \bar{x} \quad . \tag{45}$$

The radius of the arc starting from point *C* lies on the line with equation

$$\bar{y} = \bar{y}_C + \frac{\bar{y}_{S(II)} - \bar{y}_C}{\bar{x}_{S(II)} - \bar{x}_C}\left(\bar{x} - \bar{x}_C\right) \quad , \tag{46}$$

and the radius originating from point A_2 is located on the straight line

$$\bar{y} = \bar{y}_{A2} + \frac{\bar{y}_{S(II)} - \bar{y}_{A2}}{\bar{x}_{S(II)} - \bar{x}_{A2}}\left(\bar{x} - \bar{x}_{A2}\right) \quad . \tag{47}$$

The equation of *Arc II* is as follows:

$$\bar{y} = \bar{y}_{S(II)} + \sqrt{R_{(II)}^2 - \left(\bar{x} - \bar{x}_{S(II)}\right)^2} \quad . \tag{48}$$

In the example considered, $\alpha_2 = \pi/12$ rad. We therefore obtain:

$\bar{x}_{S(II)} = 0$, $\bar{y}_{S(II)} = 1{,}625.206$ m ,

$\bar{x}_C = -210.317$ m , $\bar{y}_C = 27.689$ m ,

$\bar{x}_{A2} = 210.317$ m , $\bar{y}_{A2} = 27.689$ m .

We introduce transition curves *p* and *q* in the form of a clothoid of length $L_{(II)i}$, $i = 1, 2, \ldots$ at both ends of *Arc II* (i.e., starting from points *C* and A_2). For symmetry reasons, we consider only the left half of the geometric system (with curve *p*). The segment of *Line 2* is the abscissa axis of the Cartesian coordinate system x_k, y_k, associated with the given transition curve. The origin of this system is at point *C*. We are interested in the coordinates of the endpoint of the curve in this system (i.e., point $K_{p(II)i}$). As in Chapter 6, in the equations of the transition curve, we must operate with different values of $R_{(II)i}$ of the arc radius. When using a transition curve in the form of a clothoid, equation (27) applies to $x_k(L_{(II)i})$, and equation (49) applies to $y_k(L_{(II)i})$

 doi:10.20944/preprints202512.0324.v1

$$y_k(L_{(II)i}) = \frac{L_{(II)i}^2}{6 \cdot R_{(II)i}} - \frac{L_{(II)i}^4}{336 \cdot R_{(II)i}^3} + \frac{L_{(II)i}^6}{42240 \cdot R_{(II)i}^5} \quad , \tag{49}$$

while the angle of inclination $\Theta_k(L_{(II)i})$ at the end of the curve is determined from the dependence

$$\Theta_k(L_{(II)i}) = \frac{L_{(II)i}}{2 \cdot R_{(II)i}} \quad . \tag{50}$$

The transformation of the transition curve into the $\bar{x}, \bar{y}$ coordinate system is performed by rotating the reference system by an angle $\alpha_2/2$ and shifting the curve origin to point C. The corresponding formulas depend on the direction of rotation. This operation results in the desired values of the projections of the transition curve onto the horizontal and vertical axes, which are the coordinates of the end $K_{p(II)i}$ of the curve. If the x_k, y_k system is rotated to the left (as in Figure 6), the following values are obtained:

$$\bar{x}_{Kp(II)i} = \bar{x}(L_{(II)i}) = \bar{x}_C + x_k(L_{(II)i}) \cdot \cos\frac{\alpha_2}{2} + y_k(L_{(II)i}) \cdot \sin\frac{\alpha_2}{2} \quad . \tag{51}$$

$$\bar{y}_{Kp(II)i} = \bar{y}(L_{(II)i}) = \bar{y}_C - x_k(L_{(II)i}) \cdot \sin\frac{\alpha_2}{2} + y_k(L_{(II)i}) \cdot \cos\frac{\alpha_2}{2} . \tag{52}$$

The angle of inclination $\Theta(L_{(II)i})$ at the end of the curve is determined from the relationship

$$\bar{\Theta}_{Kp(II)i} = \bar{\Theta}(L_{(II)i}) = \frac{L_{(II)i}}{2 \cdot R_{(II)i}} - \frac{\alpha_2}{2} . \tag{53}$$

Since the introduction of this transition curve is performed while maintaining the position of its starting point (i.e. point C), it is necessary to correct the position of the circular arc so that it starts at the point with coordinates $\bar{x}_{Kp(II)i}$ and $\bar{y}_{Kp(II)i}$, the angle of inclination of the tangent is there $\bar{\Theta}_{Kp(II)i}$ and the condition of symmetry of the entire system is met (i.e. $\bar{\Theta}(0) = 0$). This last condition requires the value of the arc radius to be corrected. This is directly related to the assumed length of the transition curve. Determining the corrected radius $R_{(II)i}$ requires determining the coordinates of the center $S_{(II)i}$ of the corresponding circular arc. It lies on the line perpendicular to the tangent at the end of the transition curve, with the equation

$$\bar{y}(\bar{x}) = \bar{y}_{Ka(II)i} - \frac{1}{\tan\bar{\Theta}_{Ka(II)i}}\left(\bar{x} - \bar{x}_{Ka(II)i}\right) \quad .$$

The center of the corrected circular arc lies on this line, at a distance $R_{(II)}$ from the point $K_{p(II)i}$. This gives the system of equations:

$$\bar{y}_{S(II)i} = \bar{y}_{Kp(II)i} - \frac{1}{\tan\bar{\Theta}_{Kp(II)i}}\left(\bar{x}_{S(II)i} - \bar{x}_{Kp(II)i}\right) \quad ,$$

$$\sqrt{\left(\bar{x}_{S(II)i} - \bar{x}_{Kp(II)i}\right)^2 + \left(\bar{y}_{S(II)i} - \bar{y}_{Kp(II)i}\right)^2} = R_{(II)i} \quad .$$

By solving this system of equations, we obtain the desired coordinates

$$\bar{x}_{S(II)i} = \bar{x}_{Kp(II)i} - \frac{\tan\bar{\Theta}_{Kp(II)i}}{\sqrt{1 + \left(\tan\bar{\Theta}_{Kp(II)i}\right)^2}} R_{(II)i} \quad , \tag{54}$$

$$\bar{y}_{S(II)i} = \bar{y}_{Kp(II)i} + \frac{1}{\sqrt{1 + \left(\tan\bar{\Theta}_{Kp(II)i}\right)^2}} R_{(II)i} \quad . \tag{55}$$

 doi:10.20944/preprints202512.0324.v1

The correct solution requires that the condition $\bar{x}_{S(II)i} = 0$. This means that

$$R_{(II)i} = -\frac{\sqrt{1+\left(\tan\bar{\Theta}_{Kp(II)i}\right)^2}}{\tan\bar{\Theta}_{Kp(II)i}}\bar{x}_{Kp(II)i} \quad . \tag{56}$$

In the above relation the abscissa $\bar{x}_{Kp(II)i}$ is described by formula (51), in which $x_k(L_{(II)i})$ and $y_k(L_{(II)i})$ depend on the radius $R_{(II)i}$; this also applies to the angle $\bar{\Theta}_{Kp(II)i}$.

In this situation, as in Chapter 6, the radius $R_{(II)i}$ should be determined iteratively, changing the values of this radius when determining the coordinates of point $S_{(II)i}$. The solution of the problem is determined by fulfilling the condition $\bar{x}_{S(II)i} = 0$. The final fragment of the calculations for the selected case (with $\alpha_2 = \pi/12$ rad, $x_C = -210.317$ m, $y_C = 27.689$ m and $L_{(II)i} = L_{(II)1} = 50$ m) is shown in Table 5.

Table 5. Determining the corrected radius of the second arc.

Radius $R_{(II)1}$ [m]	Abscissa $x_k(L_{(II)1})$ [m]	Ordinate $y_k(L_{(II)1})$ [m]	Angle $\Theta_k(L_{(II)1})$ [rad]	Abscissa $\bar{x}_{Kp(II)i}$ [m]	Ordinate $\bar{y}_{Kp(II)i}$ [m]	Angle $\bar{\Theta}_{Kp(II)i}$ [rad]	Abscissa $\bar{x}_{S(II)1}$ [m]	Ordinate $\bar{y}_{S(II)1}$ [m]
1421,341	49.99845	0,293144	0.017589	-160,708	21,453	-0,11331	0,000449570	1433,680
1421,340	49.99845	0,293144	0.017589	-160,708	21,453	-0,11331	0,000314437	1433,679
1421,339	49.99845	0,293144	0.017589	-160,708	21,453	-0,11331	0,000183918	1433,678
1421,338	49.99845	0,293145	0.017589	-160,708	21,453	-0,11331	**0.000053398**	**1433,677**
1421,337	49.99845	0,293145	0.017589	-160,708	21,453	-0,11331	-0.00007712	1433,676
1421,336	49.99845	0,293145	0.017589	-160,708	21,453	-0,11331	-0.00020764	1433,675
1421,335	49.99845	0,293145	0.017589	-160,708	21,453	-0,11331	-0.00033816	1433,674
1421,334	49.99845	0,293145	0.017589	-160,708	21,453	-0,11331	-0.00046868	1433,673
1421,333	49.99845	0,293145	0.017589	-160,708	21,453	-0,11331	-0.00059920	1433,672

Taking into account the appropriate number of decimal places for the determined abscissa $x_{S(II)i}$ indicated the corrected circular arc radius $R_{(II)i} = R_{(II)1} = 1421.338$ m (marked in bold in Table 5). Thus, the circular arc of radius $R_{(II)}$, which is part of the reverse arc, is replaced by a circular arc of radius $R_{(II)1}$ and two transition curves of length $L_{(II)1}$ (Figure 6).

The equation of a circular arc with radius $R_{(II)i}$ in the $\bar{x},\bar{y}$ system has the form:

$$\bar{y} = \bar{y}_{S(II)i} - \sqrt{R_{(II)i}^2 - \bar{x}^2} \quad , \qquad \bar{x} \in \langle \bar{x}_C, \bar{x}_{A2} \rangle \quad . \tag{57}$$

The entire system is described as follows:

- for $\bar{x} \in \langle \bar{x}_C, \bar{x}_{Kp(II)i} \rangle$, that is $l \in \langle 0, L_{(II)i} \rangle$

$$\bar{x}(l) = \bar{x}_C + x_k(l)\cdot\cos\frac{\alpha_2}{2} + y_k(l)\cdot\sin\frac{\alpha_2}{2} \quad ,$$

$$\bar{y}(l) = \bar{y}_C - x_k(l)\cdot\sin\frac{\alpha_2}{2} + y_k(l)\cdot\cos\frac{\alpha_2}{2} \quad ,$$

where

$$x_k(l) = l - \frac{l^5}{40\cdot R_{(II)i}^2\cdot L_{(II)i}^2} + \frac{l^9}{3{,}456\cdot R_{(II)i}^4\cdot L_{(II)i}^4} \quad ,$$

$$y_k(l) = \frac{l^3}{6\cdot R_{(II)i}\cdot L_{(II)i}} - \frac{l^7}{336\cdot R_{(II)i}^3\cdot L_{(II)i}^3} + \frac{l^{11}}{42{,}240\cdot R_{(II)i}^5\cdot L_{(II)i}^5}$$

- for $\bar{x} \in \langle \bar{x}_{Kp(II)i}, \bar{x}_{Kq(II)i} \rangle$, where $\bar{x}_{Kq(II)i} = -\bar{x}_{Kp(II)i}$

 doi:10.20944/preprints202512.0324.v1

$$\bar{y} = \bar{y}_{S(II)i} - \sqrt{R_{(II)i}^2 - \bar{x}^2}$$

- for $\bar{x} \in \langle \bar{x}_{Kq(II)i}, \bar{x}_{A2} \rangle$, that is $l \in \langle -L_{(II)i}, 0 \rangle$

$$\bar{x}(l) = \bar{x}_{A2} + x_k(l) \cdot \cos\frac{\alpha_2}{2} - y_k(l) \cdot \sin\frac{\alpha_2}{2} \quad ,$$

$$\bar{y}(l) = \bar{y}_{A2} + x_k(l) \cdot \sin\frac{\alpha_2}{2} + y_k(l) \cdot \cos\frac{\alpha_2}{2} \quad .$$

where

$$x_k(l) = l - \frac{l^5}{40 \cdot R_{(II)i}^2 \cdot L_{(II)i}^2} + \frac{l^9}{3,456 \cdot R_{(II)i}^4 \cdot L_{(II)i}^4} \quad ,$$

$$y_k(l) = -\frac{l^3}{6 \cdot R_{(II)i} \cdot L_{(II)i}} + \frac{l^7}{336 \cdot R_{(II)i}^3 \cdot L_{(II)i}^3} - \frac{l^{11}}{42,240 \cdot R_{(II)i}^5 \cdot L_{(II)i}^5} \quad .$$

In the situation shown in Figure 6, $L_{(II)i} = L_{(II)1} = 50$ m was assumed. The coordinates of the end of the first transition curve in the x_k, y_k system are as follows: $x_k(L_{(II)1}) = 49.998$ m, $y_k(L_{(II)1}) = 0.293$ m, and the angle of inclination of the tangent is $\Theta_k(L_{(II)1}) = 0.017589$ rad. For $\alpha_2 = \pi/12$ rad, $\bar{x}_C = -210.317$ m and $\bar{y}_C = 27.689$ m this corresponds to the following values in the $\bar{x}, \bar{y}$ coordinate system: $\bar{x}_{Kp(II)1} = -160.708$ m, $\bar{y}_{Kp(II)1} = 21.453$ m, $\bar{\Theta}_{Kp(II)1} = -0.11331$ rad, $\bar{x}(0) = 0$, $\bar{y}(0) = 12.339$ m, $\bar{x}_{Kq(II)1} = 160.708$ m, $\bar{y}_{Kq(II)1} = 21.453$ m, $\bar{\Theta}_{Kq(II)1} = 0.11331$ rad, $\bar{x}_{A2} = 210.317$ m and $\bar{y}_{A2} = 27.689$ m.

At the end of the discussed procedure, we transfer the obtained solution from the $\bar{x}, \bar{y}$ auxiliary coordinate system to the x, y system. To do this, we move the origin of the system to the point W_2 in the *LCS* and rotate it counterclockwise by an angle $\gamma = |\varphi_3| + \alpha_2/2$. Since in the considered case $\varphi_3 = -\pi/6$ rad, and $\alpha_2 = \pi/12$ rad, hence the angle $\gamma = 5\pi/24$ rad. The following transformation formulas apply [36]:

$$x = x_{W2} + \bar{x} \cdot \cos\gamma - \bar{y} \cdot \sin\gamma \quad , \tag{58}$$

$$y = y_{W2} - \bar{x} \cdot \sin\gamma + \bar{y} \cdot \cos\gamma \quad , \tag{59}$$

where $\gamma = |\varphi_3| + \alpha_2/2$.

8. The Resulting Geometric Arrangement of Reverse Curves

The final solution to the problem was a geometric system consisting of a circular arc of radius $R_{(I)2} = 585.697$ m with two hundred-meter transition curves in the form of a clothoid (determined in Chapter 6) and an inversely directed arc of radius $R_{(II)1} = 1421.338$ m with two fifty-meter curves in the form of a clothoid (determined in Chapter 7). The entire system is shown in Figure 7.

Preprints.org (www.preprints.org) | NOT PEER-REVIEWED | Posted: 4 December 2025 doi:10.20944/preprints202512.0324.v1

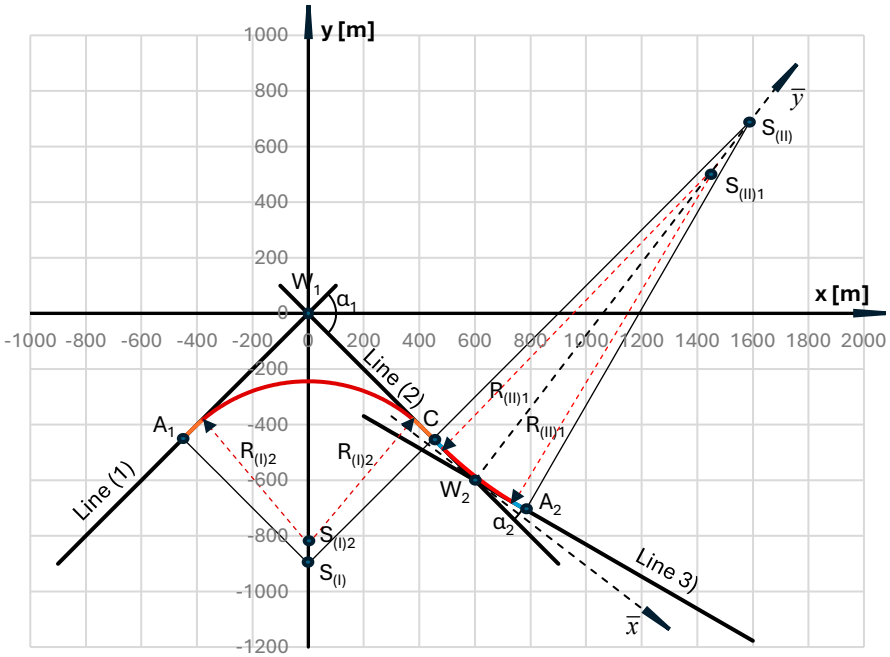

Figure 7. The determined geometric system of reverse arcs with transition curves in the local coordinate system.

After transferring the obtained solution to the PL-2000 system, using formulas (8) and (9), the situation shown in Figure 8 arises.

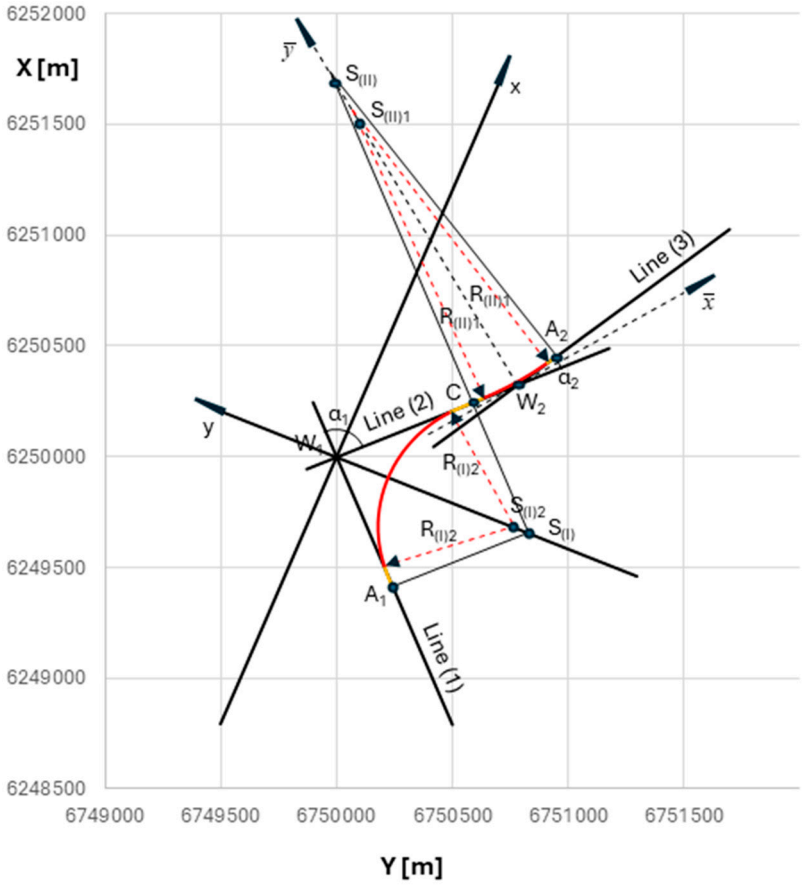

Figure 8. Designated geometric system of reverse arcs with transition curves in the PL-2000 coordinate system.

 doi:10.20944/preprints202512.0324.v1

9. Evaluation of the Obtained Solution

To evaluate the geometric system shown in Figures 7 and 8, it is necessary to first determine its horizontal curvature along its length, and then analyze the achievable train speed. The curvature diagram was based on the model of a moving rigid base of a rail vehicle, as used in Chapter 5. Figure 9 shows the curvature diagram for the resulting reverse curve system.

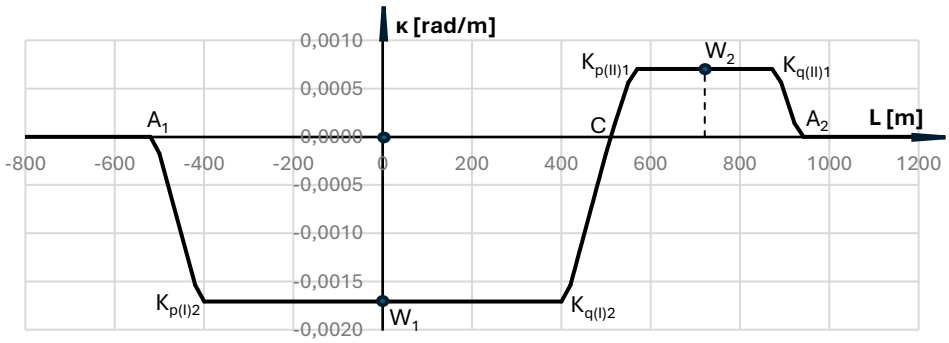

Figure 9. Graph of horizontal curvature along the length of the determined geometric system of reverse arcs from Figures 7 and 8.

The curvature diagram in Figure 9 indicates that both horizontal curves can be considered independently, and the train speed on the entire system will be determined by the curve with the greater curvature (i.e., the arc with radius $R_{(I)2}$. The first step is to check the possible speed without the use of cant. This is shown in Table 6, separately for both curves under consideration. The formulas for accelerations a_{m1} and a_{m2} from Chapter 5 (taking into account the corrected radii) and the formulas for acceleration increase

$$\psi_1 = \frac{a_{m1} \cdot V}{3,6 \cdot l_{(I)i}} \quad , \qquad \psi_2 = \frac{a_{m2} \cdot V}{3,6 \cdot l_{(II)i}} \quad .$$

Table 6. Determination of train speeds in the absence of cant for both corrected curves.

Arc with radius $R_{(I)2}$					Arc with radius $R_{(II)1}$				
V [km/h]	$R_{(I)2}$ [m]	$L_{(I)2}$ [m]	a_{m1} [m/s²]	ψ_1 [m/s³]	V [km/h]	$R_{(II)1}$ [m]	$L_{(II)1}$ [m]	a_{m2} [m/s²]	ψ_2 [m/s³]
60	585.697	100	0.47427	0.10945	90	1421.338	50	0.43973	0.30443
65	585.697	100	0.55661	0.13915	95	1421.338	50	0.48994	0.35804
70	585.697	100	0.64553	0.17380	100	1421.338	50	0.54287	0.41759
75	585.697	100	0.74105	0.21376	**105**	1421.338	50	0.59852	**0.48342**
80	585.697	100	**0.84314**	0.25943	110	1421.338	50	0.65688	0.55582
85	585.697	100	0.95183	0.31118	115	1421.338	50	0.71795	0.63511
90	585.697	100	1.06711	0.36938	120	1421.338	50	0.78174	0.72160
95	585.697	100	1.18897	0.43443	125	1421.338	50	**0.84824**	0.81561
100	585.697	100	1.31741	**0.50670**	130	1421.338	50	0.91745	0.91745
105	585.697	100	1.45249	0.58657	135	1421.338	50	0.98939	1.02744
110	585.697	100	1.59407	0.67441	140	1421.338	50	1.06403	1.14588

Table 6 shows the values of key kinematic parameters and the resulting speed derived from them. For both circular arcs, the differential impact of acceleration and acceleration increase on the achieved speed is evident. On the arc with a smaller radius (i.e. *Arc I*), the acceleration parameter plays a decisive role, determining V_{max} = 80 km/h. The acceleration gain condition would result in V_{max} = 100 km/h, but the lower value is valid. On the curve with a larger radius (i.e. *Arc II*), the opposite occurs: the acceleration gain plays a decisive role, determining V_{max} = 105 km/h (the acceleration

 doi:10.20944/preprints202512.0324.v1

condition would result in V_{max} = 125 km/h). Of course, on the entire reverse curve system, in the absence of cant, the determined speed is V_{max} = 80 km/h.

In the next step, the effects of applying cant to an arc will be examined. Table 7 presents the appropriate procedure for a circular curve with a smaller radius. The following formula for unbalanced acceleration was used:

$$a_{m1} = \frac{V^2}{(3,6)^2 R_{(I)i}} - g\frac{h_1}{s} \quad ,$$

where: h_1 – cant value in millimeters, g – acceleration of gravity (g = 9.81 m/s²), s – centre distance of rails (on standard gauge lines s = 1500 mm).

Table 7. Determining the train speed for the corrected first curve along with the selection of the cant value.

h_1 [mm]	V [km/h]	$R_{(I)2}$ [m]	$L_{(I)2}$ [m]	a_{m1} [m/s²]	ψ_1 [m/s³]	f_1 [mm/s]
120	105	585,697	100	0,66765	0,26963	35,00000
120	**110**	585,697	100	**0,80927**	0,34238	36,66667
120	115	585,697	100	0,95748	**0,42350**	38,33333
120	120	585,697	100	1,11228	0,51336	40,00000
130	105	585,697	100	0,60225	0,24322	37,91667
130	**110**	585,697	100	**0,74387**	0,31471	39,72222
130	115	585,697	100	0,89208	0,39457	41,52778
130	120	585,697	100	1,04688	**0,48317**	43,33333
130	125	585,697	100	1,20826	0,58089	45,13889
140	110	585,697	100	0,67847	0,28705	42,77778
140	**115**	585,697	100	**0,82668**	0,36565	44,72222
140	120	585,697	100	0,98148	**0,45299**	46,66667
140	125	585,697	100	1,14286	0,54945	48,61111
140	130	585,697	100	1,31083	0,65541	50,55556
145	110	585,697	100	0,64577	0,27321	44,30556
145	**115**	585,697	100	**0,79398**	0,35118	46,31944
145	120	585,697	100	0,94878	**0,43790**	**48,33333**
145	125	585,697	100	1,11016	0,53373	50,34722

The formula for the acceleration increase ψ_1 is the same as that used in Table 6, but the lifting speed of the rolling stock wheel on the gradient due to cant must be determined using the formula

$$f_1 = \frac{h_1 \cdot V}{3,6 \cdot L_{(I)i}} \quad .$$

The f_1 value should not be greater than 50 mm/s [37].

In Table 7, for each assumed cant, the key kinematic parameter values and the resulting speed are bolded. As it turns out, this speed is determined by the unbalanced acceleration occurring on the curve. The highest achievable speed on *Arc I* is 115 km/h, with an applied cant of 140 mm. For this speed, all required kinematic conditions are met.

A similar procedure performed for *Arc II* is illustrated in Table 8. The designation h_2 refers to the cant value on this curve. The following calculation formulas were used:

$$a_{m2} = \frac{V^2}{(3,6)^2 R_{(II)i}} - g\frac{h_2}{s} \quad , \qquad \psi_2 = \frac{a_{m2} \cdot V}{3,6 \cdot L_{(II)i}} \quad , \qquad f_2 = \frac{h_2 \cdot V}{3,6 \cdot L_{(II)i}} \quad .$$

In Table 8, the key values of kinematic parameters and the velocity obtained from them are also bolded. Unlike Table 7, the speed is determined by the acceleration increase on the transition curve. The highest speed achieved in this analysis on *Arc II* is 120 km/h, with a cant of 45 mm. Of course,

 doi:10.20944/preprints202512.0324.v1

this speed could be significantly increased by further increasing the cant on the curve. However, this would not make much sense, as the speed on the reverse curves will be determined by the speed on the arc with a smaller radius anyway. Therefore, in the case under consideration, trains could run at 115 km/h.

The presented procedure is universal and can be applied to other geometric situations involving the design of reverse curves. For a given layout of the main directions of a railway line, it allows for the selection of the initial radii of both circular curves, which can then be adjusted by introducing transition curves of varying lengths. The basic criterion for evaluating the resulting solution is the train speed, which can be changed by making appropriate corrections to the geometric layout.

10. Conclusions

On railway lines, due to competitive conditions with other transport systems, the most important issues currently seem to be those related to increasing train speeds; this is reflected in the dominance of high-speed rail. Traditional, existing railway lines (mostly built in the 19th century) are often overlooked in research, as they would need to be modified to meet contemporary requirements. This is particularly true for railway lines running through difficult terrain (e.g., mountainous terrain), which feature small horizontal arc radii and controversial geometric configurations such as compound curves and reverse curves. Improving the quality of these lines, leading to increased speeds, requires appropriate modernization activities.

This article addresses the design of reverse curves, a geometric system composed of two circular arcs (usually with different radii) oriented in opposite directions and directly connected. The goal is also to be able to recreate (i.e., model) an existing geometric system with reverse curves, so that subsequent corrections to the horizontal ordinates in the area where the circular arcs connect could be made. An effective design method needed to be developed that could be used not only to determine the coordinates of a new reverse curve but also to model the existing system (with a view to its subsequent modification).

The solution to the problem is obtained analytically. Individual elements of the geometric system are described using mathematical equations, and the design itself is performed in the appropriate local Cartesian coordinate system, based on the symmetrically arranged adjacent main directions of the route. However, in the case of reverse curves, there is a fundamental difference from most analytical design methods. In geometric systems, two adjacent main directions are most often identified and incorporated into further procedures (including the creation of a local coordinate system). In reverse curves, a third main direction appears, significantly complicating the matter, limiting the universality of the developed method. However, with regard to the local coordinate system, the adopted principle was retained: it is determined using two adjacent main directions. The origin of this system is located at their intersection, whose coordinates in the global coordinate system are known.

Table 8. Determining the train speed for the corrected second curve along with the selection of the cant value.

h_2 [mm]	V [km/h]	$R_{(II)1}$ [m]	$L_{(II)1}$ [m]	a_{m2} [m/s²]	ψ_2 [m/s³]	f_2 [mm/s]
20	105	1421,338	50	0,46772	0,37777	11,66667
20	**110**	1421,338	50	0,52608	**0,44514**	12,22222
20	115	1421,338	50	0,58715	0,51940	12,77778
20	120	1421,338	50	0,65094	0,60086	13,33333
20	125	1421,338	50	0,71744	0,68984	13,88889
20	130	1421,338	50	**0,78665**	0,78665	14,44444
20	135	1421,338	50	0,85859	0,89161	15,00000
30	110	1421,338	50	0,46068	0,38980	18,33333
30	**115**	1421,338	50	0,52175	**0,46155**	19,13337
30	120	1421,338	50	0,58554	0,54050	20,00000

 doi:10.20944/preprints202512.0324.v1

30	125	1421,338	50	0,65204	0,62696	20,83333
30	130	1421,338	50	0,72125	0,72125	21,66667
30	135	1421,338	50	**0,79319**	0,82369	22,50000
30	140	1421,338	50	0,86783	0,93459	23,33333
40	115	1421,338	50	0,45635	0,40369	25,55556
40	**120**	1421,338	50	0,52014	**0,48013**	26,66667
40	125	1421,338	50	0,58664	0,56408	27,77778
40	130	1421,338	50	0,65585	0,65585	28,88889
40	135	1421,338	50	0,72779	0,75578	30,00000
40	140	1421,338	50	**0,80243**	0,86416	31,11111
40	145	1421,338	50	0,87979	0,98130	32,22222
45	115	1421,338	50	0,42365	0,37477	28,75000
45	**120**	1421,338	50	0,48744	**0,44994**	30,00000
45	125	1421,338	50	0,55394	0,53263	31,25000
45	130	1421,338	50	0,62315	0,62315	32,50000
45	135	1421,338	50	0,69509	0,72182	33,75000
45	140	1421,338	50	0,76973	0,82894	35,00000
45	145	1421,338	50	**0,84709**	0,94483	36,25000
45	150	1421,338	50	0,92716	1,06980	37,50000
50	115	1421,338	50	0,39095	0,34584	31,94444
50	**120**	1421,338	50	0,45454	**0,41976**	33,33333
50	125	1421,338	50	0,52124	0,50119	34,72222
50	10	1421,338	50	0,59045	0,59045	36,11111
50	135	1421,338	50	0,66239	0,68786	37,50000
50	140	1421,338	50	0,73703	0,79372	38,88889
50	145	1421,338	50	**0,81439**	0,90836	40,27778
50	150	1421,338	50	0,89446	1,03207	41,66667

The radii of the reverse arcs must correspond to the existing system of main directions. The key issue here is to select the correct connection point for both arcs. Therefore, reverse arcs cannot be arbitrarily shaped; various conditions must be taken into account. Entering the determined arcs into the system of main directions allows for the creation of the initial geometric system of the reverse arcs. Then, transition curves are introduced for both existing circular arcs. This is possible if there is an appropriate distance between the points of intersection of the main directions (which cannot be too small). As a result, the arc radii are reduced. Their values are determined iteratively. The corresponding calculation procedure for the first arc takes place in the local coordinate system, while for the second arc in the auxiliary coordinate system, with the resulting solution subsequently transferred to the local coordinate system.

This article presents a set of formulas for creating a geometric system of reverse curves. These formulas were used in the calculation example. A graph of the horizontal curvature of the track axis and a method for determining train speed are shown. The train speed on the entire system is determined by the curve with the greater curvature. In the first stage, the achievable speed without the use of cant on the curve was determined. Next, the effects of applying cant were discussed. The presented procedure is universal and can be applied to other geometric situations involving the design of reverse curves.

Funding: This research received no external funding.

Data Availability Statement: The original contributions presented in this study are included in the article. Further inquiries can be directed to the author.

Conflicts of Interest: The author declares no conflicts of interest.

 doi:10.20944/preprints202512.0324.v1

Abbreviations

The following abbreviations are used in this manuscript:

Arc I	Marking the first circular arc
Arc II	Marking the second circular arc
A_1	Designation of the starting point of a geometric system
A_2	Designation of the end point of a geometric system
a_{m1}	Unbalanced acceleration on *Arc I*
a_{m2}	Unbalanced acceleration on *Arc II*
a_{per}	Permissible value of unbalanced acceleration
C	Destination of the assumed connection point of reverse arc
$\overline{CW_2}$	Distance between points C and W_2
f_1	Lifting speed of the rolling stock on the gradient due to cant for *Arc I*
f_2	Lifting speed of the rolling stock on the gradient due to cant for *Arc II*
g	Acceleration of gravity (g = 9.81 m/s^2)
h_1	Track cant on *Arc I*
h_2	Track cant on *Arc II*
$K_{p(I)i}$	End of the assumed transition curve before *Arc I*
$K_{p(I)1}$	End of the transition curve before *Arc I* for its assumed length $L_{(I)1}$
$K_{p(I)2}$	End of the transition curve before *Arc I* for its assumed length $L_{(I)2}$
$K_{q(I)i}$	End of the assumed transition curve after *Arc I*
$K_{q(I)1}$	End of the transition curve after *Arc I* for its assumed length $L_{(I)1}$
$K_{q(I)2}$	End of the transition curve after *Arc I* for its assumed length $L_{(I)2}$
$K_{p(II)i}$	End of the assumed transition curve before *Arc II*
$K_{p(II)1}$	End of the transition curve before *Arc II* for its assumed length $L_{(II)1}$
$K_{q(II)i}$	End of the assumed transition curve after *Arc II*
$K_{q(II)1}$	End of the transition curve after *Arc II* for its assumed length $L_{(II)1}$
l	Transition curve parameter (distance from the beginning of the curve)
l_b	Length of the rigid wagon base
LCS	Local coordinate system
Line 1	Marking the first main direction of the route
Line 2	Marking the second main direction of the route
Line 3	Marking the third main direction of the route
$L_{(I)i}$	Assumed lengths of the transition curves for *Arc I*
$L_{(I)1}$	The first assumed length of the transition curve for *Arc I*
$L_{(I)2}$	The second assumed length of the transition curve for *Arc I*
$L_{(II)i}$	Assumed lengths of the transition curves for *Arc II*
$L_{(II)1}$	The first assumed length of the transition curve for *Arc II*
p	Marking the transition curve before the circular arc
PL-2000	The Polish national spatial reference system
q	Marking the transition curve after the circular arc
$R_{(I)}$	Initial value of *Arc I* radius
$R_{(I)i}$	Corrected *Arc I* radius
$R_{(I)1}$	Value of corrected *Arc I* radius after introducing a transition curve of length $L_{(I)1}$
$R_{(I)2}$	Value of corrected *Arc I* radius after introducing a transition curve of length $L_{(I)2}$
$R_{(II)}$	Initial value of *Arc II* radius
$R_{(II)i}$	Corrected *Arc II* radius
$R_{(II)1}$	Value of corrected *Arc II* radius after introducing a transition curve of length $L_{(II)1}$
s	Centre distance of rails (on standard gauge lines s = 1500 mm)
s_1	Slope tangent *Line 1* in the *LCS*
s_2	Slope tangent *Line 2* in the *LCS*
s_3	Slope tangent *Line 3* in the *LCS*
$S_{(I)}$	Center of the primary *Arc I*
$S_{(I)i}$	Corrected *Arc I* center
$S_{(I)1}$	Corrected *Arc I* center after introducing a transition curve of length $L_{(I)1}$
$S_{(I)2}$	Corrected *Arc I* center after introducing a transition curve of length $L_{(I)2}$
$S_{(II)}$	Center of the primary *Arc II*
$S_{(II)i}$	Corrected *Arc II* center

 doi:10.20944/preprints202512.0324.v1

$S_{(II)1}$	Corrected *Arc II* center after introducing a transition curve of length $L_{(II)1}$
t_1	Value of the tangent to *Arc I*
t_2	Value of the tangent to *Arc II*
V	Train speed
V_{max}	Maximum speed of trains on the route
W_1	Intersection point of the first and second main directions of the route
W_2	Intersection point of the second and third main directions of the route
$\overline{W_1C}$	Distance between points W1 and C
$\overline{W_1W_2}$	Distance between points W1 and W2
X	North coordinate of the PL-2000 coordinate system
X_{W1}	Ordinate of point W_1 in the PL-2000 coordinate system
X_{W2}	Ordinate of point W_2 in the PL-2000 coordinate system
x	Abscissa of the local coordinate system
$\bar{x}$	Abscissa of the auxiliary coordinate system
x_{A1}	Abscissa of point A_1 in the *LCS*
x_{A2}	Abscissa of point A_2 in the *LCS*
$\bar{x}_{A2}$	Abscissa of point A_2 in the $\bar{x}, \bar{y}$ auxiliary coordinate system
x_C	Abscissa of point *C* in the *LCS*
$\bar{x}_C$	Abscissa of point *C* in the $\bar{x}, \bar{y}$ auxiliary coordinate system
x_k	Abscissa in the transition curve coordinate system
$x_{Kp(I)i}$	Abscissa of the end of the transition curve before *Arc I* in the *LCS*
$x_{Kq(I)i}$	Abscissa of the end of the transition curve after *Arc I* in the *LCS*
$\bar{x}_{Kp(II)i}$	Abscissa of point $K_{p(II)i}$ in the $\bar{x}, \bar{y}$ auxiliary coordinate system
$\bar{x}_{Kp(II)1}$	Abscissa of point $K_{p(II)1}$ in the $\bar{x}, \bar{y}$ auxiliary coordinate system
$\bar{x}_{Kq(II)i}$	Abscissa of point $K_{q(II)i}$ in the $\bar{x}, \bar{y}$ auxiliary coordinate system
$\bar{x}_{Kq(II)1}$	Abscissa of point $K_{q(II)1}$ in the $\bar{x}, \bar{y}$ auxiliary coordinate system
$x_{S(I)}$	Abscissa of the center of the primary *Arc I* in the *LCS*
$x_{S(I)i}$	Abscissa of corrected *Arc I* center in the *LCS*
$x_{S(I)1}$	Abscissa of corrected *Arc I* center in the *LCS* after introducing a transition curve of length $L_{(I)1}$
$x_{S(I)2}$	Abscissa of corrected *Arc I* center in the *LCS* after introducing a transition curve of length $L_{(I)2}$
$x_{S(II)}$	Abscissa of the center of the primary *Arc II* in the *LCS*
$\bar{x}_{S(II)}$	Abscissa of the primary center of *Arc II* in the auxiliary $\bar{x}$, $\bar{y}$ coordinate system
x_{W2}	Abscissa of point W_2 in the *LCS*
Y	Easting coordinate of the PL-2000 coordinate system
Y_{W1}	Abscissa of point W_1 in the PL-2000 coordinate system
Y_{W2}	Abscissa of point W_2 in the PL-2000 coordinate system
y	Ordinate of the local coordinate system
$\bar{y}$	Ordinate of the auxiliary coordinate system
y_{A1}	Ordinate of point A_1 in the *LCS*
y_{A2}	Ordinate of point A_2 in the *LCS*
$\bar{y}_{A2}$	Ordinate of point A_2 in the $\bar{x}, \bar{y}$ auxiliary coordinate system
y_C	Ordinate of point *C* in the *LCS*
$\bar{y}_C$	Ordinate of point *C* in the $\bar{x}, \bar{y}$ auxiliary coordinate system
y_k	Ordinate in the transition curve coordinate system
$y_{Kp(I)i}$	Ordinate of the end of the transition curve before *Arc I* in the *LCS*
$y_{Kq(I)i}$	Ordinate of the end of the transition curve after *Arc I* in the *LCS*
$\bar{y}_{Kp(II)i}$	Ordinate of point $K_{p(II)i}$ in the $\bar{x}, \bar{y}$ auxiliary coordinate system
$\bar{y}_{Kp(II)1}$	Ordinate of point $K_{p(II)1}$ in the $\bar{x}, \bar{y}$ auxiliary coordinate system
$\bar{y}_{Kq(II)i}$	Ordinate of point $K_{q(II)i}$ in the $\bar{x}, \bar{y}$ auxiliary coordinate system
$\bar{y}_{Kq(II)1}$	Ordinate of point $K_{q(II)1}$ in the $\bar{x}, \bar{y}$ auxiliary coordinate system
$y_{S(I)}$	Ordinate of the center of the primary *Arc I*
$y_{S(I)i}$	Ordinate of corrected *Arc I* center in the *LCS*
$y_{S(I)1}$	Ordinate of corrected *Arc I* center in the *LCS* after introducing a transition curve of length $L_{(I)1}$
$y_{S(I)2}$	Ordinate of corrected *Arc I* center in the *LCS* after introducing a transition curve of length $L_{(I)2}$
$y_{S(II)}$	Ordinate of the center of the primary *Arc II*

 doi:10.20944/preprints202512.0324.v1

$\overline{y}_{S(II)}$	Ordinate of the primary center of *Arc II* in the $\overline{x}, \overline{y}$ auxiliary coordinate system
y_{W2}	Ordinate of point W_2 in the *LCS*
α_1	Turning angle of the route at point W_1
α_2	Turning angle of the route at point W_2
β	Rotation angle of the PL-2000 system when transformed to the *LCS*
γ	Rotation angle of the $\overline{x}, \overline{y}$ system when it is transformed to the *LCS*
κ	Curvature of the track axis
Θ	Inclination angle at the end of the transition curve in the *LCS*
Φ_1	Inclination angle of *Line 1* in the PL-2000 coordinate system
Φ_2	Inclination angle of *Line 2* in the PL-2000 coordinate system
Φ_3	Inclination angle of *Line 3* in the PL-2000 coordinate system
Φ_x	Angle of inclination of the *x*-axis in the PL-2000 coordinate system
Φ_y	Angle of inclination of the *y*-axis in the PL-2000 coordinate system
Θ_k	Angle of inclination of the tangent at the end of the transition curve in x_k, y_k system
$\Theta_{Kp(I)i}$	Inclination angle at the end of the transition curve before *Arc I* in the *LCS*
$\Theta_{Kq(I)i}$	Inclination angle at the end of the transition curve after *Arc I* in the *LCS*
$\overline{\Theta}_{Kp(II)i}$	Angle of inclination of the tangent at the end of transition curve before *Arc II* in the $\overline{x}, \overline{y}$ coordinate system
$\overline{\Theta}_{Kp(II)1}$	Angle of inclination of the tangent at the end of transition curve of length $L_{(II)1}$ before *Arc II* in the $\overline{x}, \overline{y}$ coordinate system
$\overline{\Theta}_{Kq(II)i}$	Angle of inclination of the tangent at the end of transition curve after *Arc II* in the $\overline{x}, \overline{y}$ coordinate system
$\overline{\Theta}_{Kq(II)1}$	Angle of inclination of the tangent at the end of transition curve of length $L_{(II)1}$ after *Arc II* in the $\overline{x}, \overline{y}$ coordinate system
φ_1	Inclination angle of *Line 1* in the *LCS*
φ_2	Inclination angle of *Line 2* in the *LCS*
φ_3	Inclination angle of *Line 3* in the *LCS*
ψ	Acceleration increase
ψ_1	Acceleration increase on the transition curve for *Arc I*
ψ_2	Acceleration increase on the transition curve for *Arc II*
ψ_{per}	Permissible value of acceleration increase

References

1. Beria, P.; Grimaldi, R.; Albalate, D.; Bel, G. Delusions of success: Costs and demand of high-speed rail in Italy and Spain. *Transp. Policy* **2018**, *68*, 63–79.
2. Yang, X.; Lin, S.; Zhang, J.; He, M. Does high-speed rail promote enterprises productivity? Evidence from China. *J. Adv. Transp.* **2019**, 2019, 1, 1279489.
3. De Rus, G. The economic rationale for high-speed rail. In International Encyclopedia of Transportation, Elsevier, **2021**.
4. Xiao, F.; Wang, J.; Du, D. High-speed rail heading for innovation: The impact of HSR on intercity technology transfer. *Area Dev. Policy* **2022**, *7*, 293–311.
5. Chen, H.; Zhu, T.; Zhao, L. High-speed railway opening, industrial symbiotic agglomeration and green sustainable development – empirical evidence from China. *Sustainability* **2024**, 16(5), 2070.
6. Bigi, F.; Bosi, T.; Pineda-Jaramillo, J.; Viti, F. Long-term fleet management for freight trains: Assessing the impact of wagon maintenance through simulation of shunting policies. *J. Rail Transp. Plann. Manag.* **2024**, *29*, 100430.
7. Wang, Q.; Jiang, X.; Zeng, J.; Mao, R.; Wei, L., Wu, S. Innovative method for high-speed railway carbody vibration control caused by hunting instability using underframe suspended equipment. *JVC* **2024**, 31(15-16), 3245-3257.
8. Zhang, M.; Hu, R.; Mo, J.; Xiang, Z.; Zhou, Z. A cross-domain state monitoring method for high-speed train brake pads based on data generation under small sample conditions. *Measurement* **2024**, *226*, 114074.

 doi:10.20944/preprints202512.0324.v1

9. Qazi, A.; Yin, H.; Sebès, M.; Chollet, H.; Pozzolini, C. A semi-analytical numerical method for modelling the normal wheel-rail contact. *Veh. Syst. Dyn.* **2022**, *60*, 1322–1340.
10. Fang, C.; Jaafar, S.A.; Zhou, W.; Yan, H.; Chen, J.; Meng, X. Wheel-rail contact and friction models: A review of recent advances. *Proc. Inst. Mech. Eng. F J. Rail Rapid Transit* **2023**, 237,1245–1259.
11. Wu, B.; Yang, Y.; Xiao, G. A transient three-dimensional wheel-rail adhesion model under wet condition considering starvation and surface roughness. *Wear* **2024**, 540-541, 205263.
12. Kasimu, A.; Zhou, W.; Yan, H.; Wang, Y.; Shen, C. Evaluation of the vehicle-cargo and vehicle-trackside clearance of long and big railway freight vehicles. *Alex. Eng. J.* **2025**, 119(12), 22-34.
13. Wang, Z.; Wu, B.; Wu, S.; Wen, Z. Effects of wheel tread hollow wear on wheel-rail adhesion under wet condition. *Tribology International* **2025**, 211, 110927.
14. AutoCAD Civil 3D: Design, Engineering and Construction Software. Available online: http://www.autodesk.pl/products/civil-3d (accessed on 31 August 2025).
15. Bentley Rail Track: Rail Infrastructure Design and Optimization. Available online: https://www.bentley.com/software/rail-design (accessed on 31 August 2025).
16. Koc, W. *Elements of Track Systems Design Theory (In Polish)*; Gdansk University of Technology Publishing House: Gdansk, Poland, 2004.
17. Hodas, S. Design of railway track for speed and high-speed railways. *Procedia Eng.* **2014**, *91*, 256–261.
18. Aghastya, A.; Prihatanto, R.; Rachman, N.F.; Adi, W.T.; Astuti, S.W.; Wirawan, W.A. A new geometric planning approach for railroads based on satellite imagery. *AIP Conf. Proc.* **2023**, *2671*, 50005.
19. Guerrieri, M. Fundamentals of railway design, Chapter: The alignment design of ordinary and high-speed railways, 2023, pp. 21-56, Springer Link.
20. Tasci, L.; Kuloglu, N. Investigation of a new transition curve. *Balt. J. Road Bridge Eng.* **2011**, *6*, 23–29.
21. Kobryn, A. Universal solutions of transition curves. *J. Surv. Eng.* **2016**, *142*, 4016010.
22. Koc, W. New transition curve adapted to railway operational requirements. *J. Surv. Eng.* **2019**, *145*, 4019009.
23. Zboinski, K; Woznica, P. Optimum railway transition curves for different circular arc radii. *Arch. Civ. Eng.* **2022**, 68(4), 111-125.
24. Palsson, B.A. Design of optimization of switch rails in railway turnouts. *Veh. Sys. Dyn.* **2013**, *51*, 1610–1639.
25. Ping, W. *Design of High-Speed Railway Turnouts*; Theory and Applications; Elsevier Science & Technology: Oxford, UK, 2015.
26. Koc, W. Analytical method of connecting parallel tracks located in a circular arc using curved turnouts. *J. Transp. Eng. Part A Syst.* **2020**, *146*, 4019081.
27. Hamarat, M.; Papaelias, M.; Kaewunruen, S. Fatigue damage assessment of complex railway turnout crossings via Peridynamics-based digital twin. *Sci. Rep.* **2022**, 12(1), 14377.
28. Tonias, E.C.; Tonias, C.N. Compound and reversed curves. In *Geometric Procedures for Civil Engineers*. Springer International Publishing AG: Cham, Germany, 2016; pp. 185–242.
29. Koc W.: Design of reverse curves adapted to the satellite measurements. Adv. Civ. Eng. **2016**, 2016, 6503962.
30. Koc, W. Design of rail-track geometric systems by satellite measurement. *J. Transp. Eng.* **2012**, 138(1), 113-122.
31. Koc, W. Analytical method of modelling the geometric system of communication route. Re*MPE*, **2014**, 679817.
32. Koc, W. The analytical design method of railway route's main directions intersection area. *Open Eng.* **2016**, 6(1), 1-9.
33. Regulation of the Council of Ministers of 15 October 2012 on the national spatial reference system (in Polish). *Journal of Laws of the Republic of Poland* **2012**, position 1247.
34. Koc W.: Determination of track axis coordinates in the analytical method of designing railway route geometry. *EJAS* **2024**, 12(5), 339-362.
35. Koc, W. Modeling of compound curves on railway lines. *Geomatics* **2025**, *5*, 21.
36. Korn, G.A.; Korn, T.M. *Mathematical Handbook for Scientists and Engineers*, 1st ed.; McGraw–Hill Book Company: New York, NY, USA, 1968.

 doi:10.20944/preprints202512.0324.v1

37. Technical Standards – detailed technical conditions for the modernization or construction of railway lines up to a speed of Vmax ≤ 250 km/h. Volume I – Railroad – Appendix ST-T1-A6 – Geometric layouts of tracks (in Polish). PKP Polish Railway Lines S.A., Warszawa 2021.
38. Regulation of the Minister of Transport and Maritime Economy of 10 September 1998 on the technical conditions to be met by railway structures and their location (in Polish). *Journal of Laws of the Republic of Poland* **1998**, no. 151, position 987.